DOE/PC/94211--T4

DE-FG22-94PC94211

Co-Firing High Sulfur Coal with Refuse Derived Fuels
Technical Report #4

Wei-Ping Pan, John T. Riley, and William G. Lloyd

Center for Coal Science
and
Department of Chemistry
Western Kentucky University
Bowling Green, KY 42101

August 31, 1995

This report was prepared with the support of the U.S. Department of Energy, Grant No. De-FG22-94PC94211. However, any opinions, findings, conclusions, or recommendations expressed herein are those of the authors and do not necessarily reflect the view of the DOE. US/DOE patent clearance is not required prior to the publication of this document.

Table of Contents

1. Summary

In order to study combustion performance under conditions similar to that in the AFBC system, we conducted a series of experiments at a heating rate of 100°C/min using the TGA/FTIR/MS system. Results indicate that more hydrocarbons are evolved at the faster heating rate, owing to incomplete combustion of the fuel. Chlorinated organic compounds can be formed at high heating rates. Certain oxidation products such as organic acids and alcohols are obtained at the slow heating rate.

To simulate the conditions used in the atmospheric fluidized bed combustor (AFBC) at Western Kentucky University, studies were also conducted using a quartz tube in a tube furnace. The temperature conditions were kept identical to those of the combustor. The products evolved from the combustion of coal, PVC, and mixtures of the two were trapped in suitable solvents at different temperatures, and analyzed using the Shimadzu GC/MS system. The detection limits and the GC/MS analytical parameters were also established.

The experiments were conducted keeping in mind the broader perspective; that of studying conditions conducive to the formation of chlorinated organic compounds from the combustion of coal/MSW blends.

2. Studies with the TGA/FTIR/MS System

In previous progress reports, we reported the characteristics and thermal behavior of five raw materials and their blends at a heating rate of 10°C/min. The purpose of the experiments was to understand the progress and mechanism of thermal decomposition, the profiles for the evolution of different gaseous products, and their relative thermal stability and temperature relationships. The results are important to the analysis and control of the performance of an atmospheric fluidized bed combustor (AFBC). In order to study combustion performance under conditions similar to those for the AFBC system, we conducted a series of experiments at a heating rate of 100°C/min. By comparing the results from the two different heating rates, we hoped to see an improved picture for combustion performance during co-firing coals with refuse-derived fuels.

The thermal behavior of three additional coals, 95010 (eastern KY), 95011 (KY #9) and 95031 (IL #6), and various blends of these coals with PVC and newspaper is also included in this report.

2.1 TG/DTG Results

Table 1 summarizes the TG/DTG results at a heating rate of 100°C/min for the individual materials and their blends. On comparing the data with those at a heating rate of 10°C/min (given in report #3), we can find two obvious changes for most of the samples from the slow heating rate to the fast heating rate. The maximum rates of major weight loss (R_{max}) increase 2-8 times. Also the major decomposition temperatures (T_{max}) at R_{max} increase from 300-400°C to 350-450°C. For example, Figure 1 shows the DTG curves of coal 92073 at slow and fast heating rates, respectively. The R_{max} and T_{max} of major weight loss are 5%/min and 458°C, and 20%/min and 468°C. This indicates that the decomposition reactions of fuels occur at a faster reaction rate and higher temperature as the heating rate increases. The heating rates in an AFBC system are much faster than those in TGA experiments. Thus, we can expect decomposition reactions to occur at higher T_{max} and greater R_{max} in AFBC systems.

Figure 2 shows the DTG curves for PVC at slow and fast heating rates. The first weight loss, starting at about 263°C, represents a major decomposition stage for both heating rates. The major weight loss is 63.6%, R_{max} is 15%/min, and T_{max} is 317°C for the slow heating rate (SH). At the fast heating rate (FH), the major weight loss is 66.9%, R_{max} is 126%/min and T_{max} is 368°C. This is mainly due to the loss of HCl (57% in PVC) and the volatile matter components have small molecular weights. The second and third peaks are due to combustion of carbon skeleton chains.

For the combustion profiles of the blends, the different decomposition stages can be separated from each other only at a slow heating rate. However, it is difficult to distinguish each decomposition stage in the combustion profiles under the fast heating rate, except for the moisture loss stage. Unlike those at the slow heating rate, the profiles of decomposition reactions for blends display only one continuous weight loss at the fast heating rate.

Figures 3 and 4 are the comparison of TG curves at slow and fast heating rates, respectively, for blend 035122 and its components, coal 90003, PVC, cellulose, and newspaper. Figures 5 and 6 are the same comparison for blend 735122 and its components. It is notable that the weight losses of newspaper at T_{max} of 690°C for the slow heating rate and T_{max} of 745°C for the fast heating rate were not observed in both the blends 035122 and 735122. Actually, this pattern also occurs with all other blends using newspaper at both heating rates. This may be due to some reactions between coal and the residue of newspaper to form volatile products at a lower temperature. For the slow heating rate, the blends decompose before the majority of their components, as shown in Figure 3 for 035122 and Figure 5 for 735122. For the fast heating rate, the major decomposition stages of blends are in between those of the components as shown in Figure 4 for 035122 and in Figure 6 for 735122. Decomposition of the blend is later than cellulose and newspaper, and earlier than PVC and coal. This indicates that combustion behavior differs in the slow and fast heating rates.

Figure 7 is a comparison for the combustion profiles of coals 95010, 95011, 95031, 92073 and 90003 at the slow heating rate. It is indicated that the combustion behavior of these coals are very similar, except for greater ash residue in coal 92073.

2.2 FTIR Results

In order to easily identify data in tables, we have defined files having an prefix "H-" in the filename as being at the fast heating rate, the rest of the files are at the slow heating rate. The construction of a file name is the same as that used in report #2.

2.2.1 Results at the Fast Heating Rate

Figure 8 shows 3D FTIR spectra of PVC decomposition products at the fast heating rate. At the slow heating rate (as reported in report #3) the first decomposition phase (Z = 500-1500) consists of HCl, benzene and oxidized organic products (organic acids and alcohols). The second phase (Z=1500-3000) is mainly completely oxidized products of the carbon chain, such as carbon dioxide, carbon monoxide and water, along with small amounts of methane and tar. In Figure 8, the gaseous products are evolved in a much narrower temperature range. Therefore, it is difficult to identify the decomposition products for the different stages. Thus, the two thermal decomposition stages observed at the slow heating rate were not observed at the fast heating rate.

There are two important characteristics shown in Figure 8. One is the shift of absorbance curves due to the evolution of a lot of gaseous decomposition products into the FTIR cell in a short time. The other is the appearance of peaks near 1000, 1750, and 3000 cm^{-1}, which occur after the rapid decomposition of fuels and always occur at almost the same wavenumber. We cannot identify the source of these peaks with certainty. It is possible that these peaks come from some kind of high molecular weight aliphatic acids formed by the rapid decomposition of carbon skeletons. The peak at 1000 cm^{-1} is due to the out-of-plane bending of the C-H bonds. Similar results can be seen in the FTIR spectra from newspaper and cellulose at the fast heating rate. By comparison, 3D FTIR spectra of newspaper decomposition is shown in Figure 9.

Figure 10 shows 3D FTIR spectra of decomposition products of coal 92073 at the fast heating rate. Unlike the three peaks that appear for different sulfur forms in the profile of sulfur dioxide at the slow heating rate, only one overlapping peak of sulfur dioxide is observed, along with other gases at the fast heating rate. This change indicates that the oxidative decomposition of different sulfur forms occurs in a narrow temperature range, except for sulfate sulfur, which decomposes continuously and slowly over a long range.

Figure 11 shows a 3D FTIR spectra for decomposition products of blend mixture 735122 at the fast heating rate. A trend similar to the slow heating rate is observed. At the slow heating rate carbon monoxide always evolves along with carbon dioxide. There is only a small amount of methane released at the higher temperature after HCl is evolved. On the other hand, at the fast heating rate carbon monoxide appears only at the very beginning. Also, enhanced methane evolution is released at the same time as the evolution of HCl. The greater amount of methane produced at the fast heating rate may be due to the incomplete combustion of fuels.

Table 2 is a summary of the tentative identification of FTIR peaks for raw materials at the slow and fast heating rates. More than 15 kinds of gaseous species can be identified. The data indicates that at the fast heating rate, it is easier to find methane and xylenes in the evolved gases. At the slow rate, more oxidation products such as acids and alcohols are found. For coals, peaks between 1700-1800 cm^{-1} can be observed. However, they are not strong enough to be distinguished from the water peaks. The peaks at 741 cm^{-1} can be assigned to either chlorobenzene or o-xylene. But in the cases of "Hnewspaper" and "Hcellulose", it is more likely that the peak could be o-xylene because there is no detectable chlorine in newspaper and cellulose as indicated from the elemental analysis of the materials. For the identification of hydrogen cyanide, the stretching vibration of the C-H bond, a doublet peak at 3330 and 3280 cm^{-1}, is important evidence besides the bending absorption at 712 cm^{-1}.

Tables 3 and 4 are summaries of tentative identification of FTIR peaks for combustion products of 92073 blends and 90003 blends at both heating rates.

From all the FTIR data, it is indicated that more hydrocarbon gases are produced at the fast heating rate due to incomplete combustion of fuels. Certain oxidation products such as organic acids and alcohols are obtained at the slow heating rate.

2.2.2 FTIR Results from Coals 95010, 95011, and 95031

Figures 12-14 show 3D FTIR spectra for the decomposition products of coals 95010, 95011, and 95031 at the slow heating rate. They are similar to those of coals 90003 and 92073. From the profiles of sulfur dioxide (1374 cm^{-1}), we can see that there is much higher sulfur content in coal 95031 and 95011 than in coal 95010. as shown in the FTIR spectra from coal 95010, more tar was detected after 400°C due to the high fixed carbon content in the matrix of this coal. Figures 15-17 show 3D FTIR spectra for the combustion products from blends of the coals at the slow heating rate. The samples are made up of 50% coal, 25% PVC, and 25% newspaper. The HCl evolution is much earlier than that of methane. The results are similar to those for coals 90003 and 92073.

Figures 18-20 show 3D FTIR spectra for the decomposition products of coals 95010, 95011, and 95031 at the fast heating rate. Figures 21-23 show spectra for their mixtures with PVC and newspaper at the fast heating rate. Compared with the graphs from the slow heating rate, the FTIR spectra at the fast heating rate display much more and stronger hydrocarbon peaks near 3000 cm^{-1}.

Tables 5 and 6 are summaries for the identified peaks in the twelve 3D spectra listed above. From the data for HCl and sulfur dioxide, coal 95031 is a high chlorine and high sulfur bituminous coal.

In summary, the chlorine and hydrocarbon species formed during the combustion of blends are released at the same time for the fast heating rate whereas they evolve at different times for the slow heating rate. Also, it is demonstrated that more hydrocarbons are produced at the fast heating rate. These results indicate there are more opportunities and a greater possibility for yielding harmful chlorinated organic compounds during co-firing coals with refuse derived fuels at the faster heating rate that may occur in an AFBC system.

2.3 Mass Spectral Results

Because many species in the gaseous combustion mixtures can not be identified or even detected using an FTIR, we have to use a mass spectrometer (MS) as a method complementary to the FTIR. As with the FTIR, MS results from the fast heating rate show the same trend in which the decomposition reactions are compressed into a narrow time range during the heating process. Thus the decomposition stages of different components cannot be separated. This make our analysis complicated although it simulates the combustion conditions in the AFBC system more closely. Therefore, we attempt only to compare and discuss the changes resulting from different heating rates, and finally try to tentatively identify some of the major mass peaks of all files in this report.

Figures 24 and 25 are the profiles of some major peaks for PVC at the slow heating rate. Figure 24 is for HCl (mass 36), molecule chlorine (mass 70), chlorobenzene (mass 112), and their isotopic peaks (38, 72, 74, and 114). Their peak area integration ratios are close to the theoretical chlorine isotopical fraction. The same results can be obtained from the PVC fast heating rate (Figure 26). Figure 25 shows that benzene (78) and naphthalene (128) appear early with the chlorine species. This is supported by FTIR results of PVC as previously discussed. The profiles mass units 105 and 106 have the same shapes and intensities. This indicates that they may be due to the same species. Therefore, we tentatively identify them as benzaldehyde and benzaldehyde-H, or xylene and xylene-H, or ethylbenzene and ethylbenzene-H. Both of the species must have identical thermal stability. This is possible in the ionization environment of the MS.

Figure 27 shows the profiles of some peaks for coal 92073 at the fast heating rate. The peaks, which are for water, oxygen, carbon dioxide, carbonyl sulfide and sulfur dioxide at the slow heating rate can be explained as previously discussed in report #3. At the fast heating rate, however, these peaks do not display the same trends that were observed at the slow heating rate.

This may be due to partial pyrolysis at high temperatures to produce many complex species with small masses.

Figure 28 shows the profiles for file 035122 at the slow heating rate. The peaks 60 (carbonyl sulfide) and 64 (sulfur dioxide) display the same changes observed in coal 92073. Sulfur dioxide has three decomposition phases and carbonyl sulfide has only two. In the profiles for HCl, molecular chlorine and chlorobenzene, there are some changes. HCl and molecular chlorine show two peaks. From the decomposition temperature and intensity ratio of isotopical peaks, the first HCl peak may be attributed to the decomposition of PVC. The second peak is due to the decomposition of coal and PVC. In addition, we cannot see the isotopical peak (114) of chlorobenezene (112). Peak 112 is the largest one detected in this file. Figure 29 shows some profiles for file H035122 at the fast heating rate. In this figure sulfur dioxide does not display the three decomposition steps, and the peaks 36/38, 70/72/74, and 112/114 do not display the expected ratio. This may be due to the complexity of the reactions at high temperatures. Figures 30 and 31 are some profiles for mixture 735122 at the slow and fast heating rates. They display similar results to those obtained with blend 035122.

Tables 7, 8, and 9 summarize the tentative identification of major peaks in the MS files for both the individual components and mixtures at the slow and rapid heating rates. There are more than 20 detectable organic compounds in the evolved gases. Most of these materials are aromatic compounds. Some of them, the compounds in bold type, were also identified in the GC/MS experiments with gases trapped in solution (see next section). It is notable that peak 112 in the spectra of blends appears more often at the fast heating rate than slow heating rate. In accordance with the FTIR data, this is probably an indication that chlorinated organic compounds can be formed more easily at the fast heating rate.

3. Studies with the Tubular Furnace

The materials used for the study were coal #92073 (high sulfur, low chlorine coal) and pure PVC resin from Oxy Chem, Ltd.

Previous attempts had met with little success, so the main priority of this renewed effort was to study the reasons for the lack of data and adopt remedial measures.

The most puzzling fact was that combustion studies using the TG/FTIR/MS system yielded certain results while similar studies done with the GC/MS system would not. The main difference in the techniques lays in the fact that while the TG/FTIR/MS was essentially an "on line" analysis, the GC/MS system was not. The heart of the problem lay in the manner of sample collection.

To confirm suspicions, it was decided to burn known components, collect them in the traps and analyze them using the GC/MS. There was also the question of a suitable solvent. Candidate solvents were toluene and methylene chloride. These were chosen based on the literature published on related topics. From an exhaustive study of the literature a list of the most commonly reported compounds (from the combustion of coal and PVC individually) was

compiled. The list consisted mainly of polyaromatic hydrocarbons containing highly compact ring systems[1,2] (See Tables 10 and 10-1).

The compounds chosen as standards for the study were naphthalene (bp = 218°C), 2-methylanthracene (bp = 196°C) and fluorene (bp = 293°C). They were chosen for two main reasons:

(a) Relevance (most often reported from coal combustion)
(b) The wide range of boiling points.

3.1 Experimental Setup

A twelve-inch quartz tube furnace with a teflon coated end (which was in contact with the solvent) was used. Air was used as the carrier gas, and the flow rate was initially kept at 17 mL/min (calculated by calibrating the flow meter), as illustrated in Figure 32.

3.2 Establishing Detection Limits and GC/MS Analysis Parameters

First a solution containing 50 mg of each of the chosen standards was prepared in 250 mL of toluene. This was analyzed using the GC/MS. The analysis parameters used are given in Table 11. Since the components were detected without any problem (due to good resolution), it was decided to use the same compounds for analysis of the components in the trap.

A 50 mg sample of each component (naphthalene, 2-methyl anthracene, fluorene) was weighed, crushed, powdered, and placed in a porcelain boat. Air (15 mL/min) was used as the carrier gas. A 25 mL portion of toluene (previously dried over anhydrous magnesium sulphate and filtered through a 0.5μ filter) was used as the solvent. Since toluene is not a very volatile solvent, the coolant used was cold water (near 0°C).

The furnace was heated gradually from room temperature to 400°C (greater than the boiling point of the highest boiling component). There was a problem, however. The vapors condensed in the cooler parts of the furnace and only a small fraction actually went into the trap solution. To overcome this problem a heating tape was used. The temperature of the tape was kept at 250°C, the maximum temperature that the teflon tube could withstand. This prevented the vapors from condensing, but gave rise to huge peaks of di-n-octyl phthalate on subsequent analysis.

The vapors collected were then analyzed using the GC/MS. All three components could be detected with ease. This indicated that the setup was free of major problems.

The next step was to determine detection limits. The amount of each chosen standard was successively reduced from 50 mg to 30 and then 10 mg. At each stage, it was possible to trap the vapors and detect the components easily. The amount used was then reduced to 1 mg of each

component. The ensuing vapors were then trapped in about 5 mL of the solvent, but the ease of detection was lowered considerably. (Table 12).

3.3 Studies with Raw Materials

3.3.1 Studies Using PVC

Since the procedure for collecting vapors from the tubular furnace had improved, actual samples, namely PVC and coal were burned and analyzed individually.

Pure PVC resin supplied by Oxy Chem, Ltd. was used for the study. Earlier studies done using the TG/FTIR/MS system for the combustion of PVC had shown HCl, benzene, toluene, styrene and other alkyl benzenes as evolved products. Since HCl is soluble in aqueous media and the other components more soluble in organic solvents, two traps were used. A long thin column packed with glass beads (to increase surface area) and 2% $NaHCO_3$ was used as the first trap. It was chilled using liquid nitrogen (approximately -178°C). The second trap used toluene as solvent and dry ice as coolant (approximately - 70°C). Initially, 5 g of PVC was burned in an air flow of about 17 mL/min. The sample was heated gradually from room temperature to 700°C (the decomposition temperature). The vapors were analyzed using the GC/MS system. It was possible to detect components such as styrene and naphthalene from the toluene trap. The inability of the system to detect benzene lay in the fact that benzene had a shorter retention time as compared to toluene. It was obvious that a more volatile solvent would be necessary and methylene chloride was the obvious choice. Analysis of the aqueous trap yielded HCl and trace amounts of styrene as the only components.

The above procedure was repeated using methylene chloride as solvent in the second trap, instead of toluene. In this case, peaks detected were benzene, toluene and styrene.

The amount of PVC burned was lowered successively to one gram. It was possible to detect the above mentioned compounds with relative ease. For amounts below one gram, there were problems associated with analysis parameters such as detector voltage and baseline noise; identities could not be verified with a reasonablely high similarity index. (Table 13)

3.3.2 Studies Using Coal #92073

This coal is a high sulfur, low chlorine content coal. Since in the PVC studies methylene chloride had proved to be a good solvent, it was decided to use the same solvent for coal combustion studies.

The experimental setup remained the same; only the sample was changed from PVC to 5 g of coal. Chromatographic analysis yielded a number of linear alkanes and alkylbenzenes as the major products. Effects on the trapped components and the relationship with the coolants used, if any, were studied. The coolants used ranged from liquid nitrogen at the coldest (approximately -

170°C) to ice cold water (0°C) at the warmest. Other coolants used were dry ice (approximately -77°C) and ice and calcium chloride freezing mixture (approximately -30°C). Each of the samples was analyzed using the same chromatographic technique. There was no appreciable change in the results thus obtained.

To avoid problems of tar formation and reduce the possibility of pyrolysis, air flow was increased to one standard cubic foot per hour (SCFH), i.e., approximately 470 mL/ min. Also, in order to reproduce the conditions of the AFBC unit, the sample tube was introduced only after the furnace had reached 800°C. The same was done to the PVC sample. The summary of the results obtained are included in Table 14. The GC/MS temperature program and analytical parameters are in given in Table 15.

In all of the studies conducted thus far, a quartz furnace with an outer diameter of 12 inches was used. Being thick walled, this significantly reduced the inner diameter at the outlet and resulted in clogging at the point of entry of vapors into the solvent, possibly due to the large temperature difference. To overcome this, quartz tubes with inner diameters of one quarter inch at the outlet are being used for current studies. Instead of using glass beads to increase surface area, a Tenax trap was used, as this resin is especially suited to adsorption of volatile organic compounds.

A protocol for positive identification of compounds by the GC/MS analysis has been established. The details are summarized in Table 16.

Studies are still being conducted to improve the technique for trapping the volatile organic compounds evolved during combustion. Future research will focus on analysis of compounds evolved due to combustion of municipal solid waste, newspaper, cellulose and their combinations with coal and PVC.

4. Fluidized Bed Combustion

Two preliminary AFBC runs were made on June 22nd and July 21st. The purpose of these runs was to explore the effects of fuel/air ratio on the flue gas composition. The results of the June 22 burn show that:

1. The bed heat exchange tubes have been able to absorb around 120,000 BTU/hr heat. Thus the bed temperature can be easily controlled when changing the air fuel ratio during combustion.

2. The CO_2 concentration in the flue gas reached around 14% at port 2 (about 73" above the setter plate).

3. Port 2 and port 1 (101 7/8" above the setter plate) have very similar compositions, indicating that the leak between port 1 and port 2 has been substantially closed.

4. Port 3 (36" above the setter plate) was too close to the bed and the gas composition was not consistent. It will be moved to a new position (about 50" above the setter plate) for the next test run.

5. A better control of the secondary and primary air flow is needed for the next test run. This modification will help in reaching the desired gas composition (around 16% CO_2 and 5% O_2).

The purposes of the July 21st were:

1. To test the newly arrived limestone (Kentucky limestone from Princeton, KY) which has been used at the Paducah TVA power plant.

2. To test the modified control system for the primary and secondary air.

3. To test the new sampling port #3 (around 50" above the setter plate)

However, this run failed due to the large amount of limestone dust present. At this time, preparation of the correct particle size distribution for the limestone is underway.

5. Acknowledgements

We are pleased to acknowledge the valuable help of our student assistants and visiting scholars.

Undergraduate Students (Chemistry)

John Napier

Graduate Students (Chemistry)

Jessica Yin
Richard Lu
Jenny Heidbrink
Shobha Purushothama
Xiaodong Yang

Visiting Scholars

Hongtao Zhang
Hanxu Li

UCR Program Participant

John D. Hyatt
Centenary College, Louisiana

Table 1. Summary of TG/DTG Results at Fast Heating Rate
(100°C/min to 900°C; Isothermal for 5 Minutes in Air 50 mL/min)

Sample	ΔW_1(%)	T_{max}	R_{max}	ΔW_2(%)	T_{max}	R_{max}	ΔW_3(%)	T_{max}	R_{max}
HPVC	66.9	368	126	18.2	450	28.1	14.9	653	9.4
H90003	0.6	160	1	90	486	22			
H92073	5.2	128	4.4	70.2	468	20			
Hnewspaper				91.4	395	168	1.7	745	2.9
Hcellulose	94.3	408	183	3.4	534	11.3	2.3	585	5.8
H03PVC50				41.7	354	71	54.9	435	32
H03NEW50	3.4	106	2.7	93	349	41			
H03CEL50	2.9	112	2.9	92.3	361	67			
H03P2N25	1.8	102	1.3	94.1	345	81			
H035122	1.3	122	1.4	94.3	357	107			
H73PVC50	2.5	113	1.9	82.3	347	57			
H73NEW50	4.3	103	4.0	72.8	374	99			
H73CEL50	4.3	109	3.3	81.7	383	99			
H73P2N25	2.5	100	2.29	85.1	344	98			
H735122	3.1	98	2.4	91	363	160			

Note: R_{max} is maximum rate of weight loss, %/min; T_{max} is the temperature at R_{max}, °C.

Table 2. Tentative Identification of FTIR Peaks for Raw Materials (wavenumber, cm^{-1})

Name	PVC	HPVC	Newsp	Hnews	Cellulos	Hcellul	90003	H90003	92073	H92073
methane	3016	3016	-	3016	-	3016	3016	3016	3016	3016
hydrogen chloride	2798	2798	-	-	-	-	2798	2798	2798	2798
carbon dioxide	2358	2358	2358	2358	2358	2360	2358	2360	2358	2360
carbon monoxide	2178	2178	2178	2178	2178	2178	2178	2176	2178	2178
carbonyl sulfide	-	-	-	-	-	-	2073	2074	2073	2074
carbonyl group (multiplet)	1800~ 1700	1800~ 1700	1800~ 1700	1800~ 1700	1800~ 1700	1800~ 1700	?	?	?	?
sulfur dioxide	-	-	-	-	-	-	1374	-	1374	1374
acetic acid	1175	-	1175	-	1175	1174	-	1175	-	-
formic acid	1106	-	1107	-	1107	1107	-	1106	-	-
methanol	1033	-	1034	-	-	-	-	-	-	-
ethylene	950	950	950	950	950	950	950	950	950	950
propylene	-	-	-	-	-	-	-	-	-	912
1,3-butadiene	908	908	-	-	-	908	908	909	909	-
p-Xylene	-	-	-	-	-	-	-	794	-	793
furan	-	-	745	745	744	744	-	-	-	-
chlorobenzene or o-Xylene	741	741	-	741	-	741	741	741	741	741
hydrogen cyanide (3330,3280D)	-	-	-	-	-	-	712	712	712	712
benzene	674	674	-	-	-	-	-	-	-	-

Table 3. Tentative Identification of FTIR Peaks for Coal 92073 Mixtures (wavenumber, cm^{-1})

Name	73PVC	H73PV	73New	H73Ne	73Cell	H73Cell	73P2N2	H73PN	735122	H73122
methane	3018	3016	3016	3016	3018	3016	3016	3016	3016	3016
hydrogen chloride	2798	2798	2798	2798	2798	2798	2798	2798	2798	2798
carbon dioxide	2358	2358	2358	2358	2358	2358	2358	2358	2358	2360
carbon monoxide	2178	2178	2178	2178	2178	2178	2178	2178	2178	2178
carbonyl sulfide	2074	2074	2074	2074	2074	2074	2074	2074	2074	2074
carbonyl group (multiplet)	1800~ 1700	1800~ 1700	1800~ 1700	1800~ 1700	1800~ 1700	1800~ 1700	1800~ 1700	1800~ 1700	1800~ 1700	1800~ 1700
sulfur dioxide	1374	1374	1374	1374	1374	1374	1374	1374	1374	1374
acetic acid	1175	-	1175	1175	1175	-	1175	1176	1176	-
formic acid	1107	-	1107	1107	1107	1107	1107	1107	1107	1106
methanol	-	1034	1034	1033	-	1033	-	1033	-	-
ethylene	950	950	-	950	950	950	950	950	950	950
1,3-butadiene	908	-	-	908	908	-	908	908	906	-
p-Xylene	793	-	-	793	-	-	-	793	-	793
furan	-	-	745	745	745	745	745	745	745	745
chlorobenzene or o-Xylene	741	741	741	741	741	741	741	741	741	741
hydrogen cyanide (3330,3280D)	712	-	712	-	712	-	712	-	712	712

Table 4. Tentative Identification of FTIR Peaks for Coal 90003 Mixtures (wavenumber, cm^{-1})

Name	03PVC	H03PV	03New	H03Ne	03Cell	H03Cell	03P2N2	H03PN	035122	H03122
methane	3018	3016	3016	3016	3018	3016	3016	3016	3016	3016
hydrogen chloride	2798	2798	2798	2798	2798	2798	2798	2798	2798	2798
carbon dioxide	2358	2358	2358	2358	2358	2358	2358	2358	2358	2360
carbon monoxide	2178	2178	2178	2178	2178	2178	2178	2178	2178	2178
carbonyl sulfide	2074	2074	2074	-	2074	-	2074	-	2074	-
carbonyl group (multiplet)	1800~ 1700	1800~ 1700	1800~ 1700	1800~ 1700	1800~ 1700	1800~ 1700	1800~ 1700	1800~ 1700	1800~ 1700	1800~ 1700
sulfur dioxide	1374	1374	1374	-	1374	-	1374	-	1374	-
acetic acid	1175	-	1175	-	1175	1174	1175	1175	1176	1176
formic acid	-	-	1107	1107	1107	1107	1107	1106	1107	1106
methanol	-	1034	1034	1033	1033	-	1033	1033	1033	1033
ethylene	950	950	-	950	-	950	950	950	950	950
1,3-butadiene	908	908	-	-	-	-	-	908	-	908
isoprene	-	-	-	-	-	-	-	-	-	894
furan	-	-	745	745	745	744	745	745	745	745
chlorobenzene or o-Xylene	741	741	741	741	741	741	741	741	741	741
acetylene	-	-	-	-	-	-	-	-	-	730
hydrogen cyanide (3330,3280D)	712	-	712	-	712	-	712	712	712	712

Table 5. Tentative Identification of FTIR Peaks for Coals 95010, 95011, and 95031 Heated at 10°C/min to 700°C in Air 50 mL/min (wavenumber, cm^{-1})

Name	95010	95011	95031	10P2N2	11P2N2	31P2N2
methane	3018	3016	3016	3016	3018	3016
hydrogen chloride	2798	-	2798	2798	2798	2798
carbon dioxide	2358	2358	2358	2358	2358	2358
carbon monoxide	2178	2178	2178	2178	2178	2178
carbonyl sulfide	-	2074	2074	-	2074	2074
carbonyl group (multiplet)	?	?	?	1800~ 1700	1800~ 1700	1800~ 1700
sulfur dioxide	-	1374	1374	-	1374	1374
acetic acid	1175	1175	1175	1175	1175	1175
formic acid	1107	1107	1107	1107	1107	1107
methanol	-	-	-	1033	1033	-
ethylene	950	950	950	950	950	950
1,3-butadiene	-	907	907	908	908	-
p-Xylene	793	793	793	793	-	-
furan	-	-	-	745	745	745
o-xylene or chlorobenzene	741	741	741	741	741	741
hydrogen cyanide (3330,3280D)	712	713	712	712	712	712

Table 6. Tentative Identification of FTIR Peaks for Coals 95010, 95011, and 95031
Heated at 100°C/min to 700°C, Isothermal for 20 Minutes in Air 50 mL/min (wavenumber, cm^{-1})

Name	H95010	H95011	H95031	H10P2N2	H11P2N2	H31P2N2
methane	3018	3016	3016	3016	3018	3016
hydrogen chloride	-	-	2798	2798	2798	2798
carbon dioxide	2358	2358	2358	2358	2358	2358
carbon monoxide	2178	2178	2178	2178	2178	2178
carbonyl sulfide	-	2074	2074	-	2074	2074
carbonyl group (multiplet)	?	?	?	1800~ 1700	1800~ 1700	1800~ 1700
sulfur dioxide	-	1374	1374	-	1374	1374
ethyl acetate	-	-	-	-	1245	-
ethyl formate	1185	-	-	1185	-	-
acetic acid	1175	1175	1175	1175	1175	1175
formic acid	1107	-	-	1107	1107	1107
methanol	-	-	-	-	1033	1033
ethylene	950	950	950	950	950	950
propylene	912	912	-	-	-	-
1,3-butadiene	-	907	907	-	907	-
p-Xylene	793	793	793	-	-	-
furan	-	-	-	745	745	745
o-xylene or chlorobenzene	741	741	741	741	741	741
hydrogen cyanide (3330,3280D)	712	713	712	712	712	712
benzene				674	674	

Table 7. Tentative Parent Structures of MS Peaks

Name	PVC	HPVC	Newsp	HNews	Cellulos	HCellul	90003	H90003	92073	H92073
benzofluorene	216									
methylfluoranthene	216									
methylpyrene	216									
hydroxydibenzofuran-H									183	
methyldibenzofuran	182									
trihydroxynaphthalene		176								
chloroquinoline									163	
1,4-naphthoquinone		158								
dimethylnaphthalene		156								
vinylnaphthalene		154								
acenaphthene		154								
biphenyl		154								
dichlorobenzene	146	146								
indan-1,3-dione	146	146								
methyltetrahydronaphthalene	146	146								
methylnaphthalene		142								
methylnaphthalene-H									141	
methyl benzoate									136	
ethylindole			131							
naphthalene	128	128								
trimethylcyclohexane	126	126								
benzodihydrofuran	120	120	120	120				120	120	
propylbenzene	120	120	120	120				120	120	
acetophenone	120	120	120	120				120	120	
methylbenzaldehyde	120	120	120	120				120	120	
trimethylbenzene	120	120	120	120				120	120	
indoline	119	119	119	119				119		
chlorobenzene	112	112						112	112	112
dimethylcyclohexane	112	112						112	112	112
5-methylfurfural			110			110				
anisole									108	
cresol									108	
methylphenol									108	
xylene	106	106	106	106				106		106
benzaldehyde	106	106	106	106				106		106
ethylbenzene	106	106	106	106				106		106
xylene-H	105	105	105	105	105	105	105	105		105
benzaldehyde-H	105	105	105	105	105	105	105	105		105
3-methyl-2-furanone	98	98	98	98	98	98	98	98	98	98
methylthiophene	98	98	98	98	98	98	98	98	98	98
furfural	96	96	96	96	96	96		96		96
furfural-H	95	95	95	95	95	95	95	95		95
toluene	92	92	92	92	92	92	92	92	92	92
toluene-H	91	91	91	91	91	91	91	91	91	91
hexene	84	84	84	84	84	84	84	84	84	84
thiophene							84	84	84	84
methylfuran			82	82	82	82	82	82		
benzene	78	78	78	78	78	78	78	78	78	78
furan			68	68	68	68	68	68		
sulfur dioxide							64	64	64	64

Table 8. Tentative Parent Structures of MS Peaks

Name	73PVC	H73PV	73New	H73Ne	73Cell	H73Cell	73P2N2	H73PN	735122	H73122
dimethylnaphthalene		156								
vinylnaphthalene		154								
acenaphthene		154								
biphenyl		154								
methylbenzothiophene	148						148	148	148	
phthalic anhydride	148						148	148	148	
dichlorobenzene	146						146	146	146	
indan-1,3-dione	146						146	146	146	
methyltetrahydronaphthalene	146						146	146	146	
methylnaphthalene		142					142	142	142	
chlorobenzaldehyde		140					140	140	140	
chlorobenzaldehyde-H		139					139	139	139	
benzothiophene	134	134	134				134	134	134	
naphthalene	128	128	128				128	128	128	
trimethylcyclohexane	126	126					126	126	126	
benzodihydrofuran	120	120	120				120	120	120	120
propylbenzene	120	120	120				120	120	120	120
acetophenone	120	120	120				120	120	120	120
methylbenzaldehyde	120	120	120				120	120	120	120
trimethylbenzene	120	120	120				120	120	120	120
chlorobenzene	112	112	112	112		112	112	112	112	112
dimethylcyclohexane	112	112	112	112		112	112	112	112	112
xylene	106	106	106	106	106	106	106	106	106	106
benzaldehyde	106	106	106	106	106	106	106	106	106	106
ethylbenzene	106	106	106	106	106	106	106	106	106	106
xylene-H	105	105	105	105	105	105	105	105	105	105
benzaldehyde-H	105	105	105	105	105	105	105	105	105	105
3-methyl-2-furanone	98	98	98	98	98	98	98	98	98	98
methylthiophene	98	98	98	98	98	98	98	98	98	98
furfural	96	96	96	96	96	96	96	96	96	96
toluene	92	92	92	92	92	92	92	92	92	92
toluene-H	91	91	91	91	91	91	91	91	91	91
hexene	84	84	84	84	84	84	84	84	84	84
thiophene	84	84	84	84	84	84	84	84	84	84
benzene	78	78	78	78	78	78	78	78	78	78
furan	68	68	68	68	68	68	68	68	68	68
sulfur dioxide	64	64	64	64	64	64	64	64	64	64

Table 9. Tentative Parent Structures of MS Peaks

Name	03PVC	H03PV	03New	H03Ne	03Cell	H03Cell	03P2N2	H03PN	035122	H03122
vinylnaphthalene		154								
acenaphthene		154								
biphenyl		154								
methylnaphthalene		142								
chlorobenzaldehyde		140						140		
chlorobenzaldehyde-H		139								
benzothiophene		134								
naphthalene	128	128					128	128		
trimethylcyclohexane		126				126		126		
benzodihydrofuran		120		120				120		120
propylbenzene		120		120				120		120
acetophenone		120		120				120		120
methylbenzaldehyde		120		120				120		120
trimethylbenzene		120		120				120		120
indoline		119		119			119	119		119
octane	114	114				114	114	114		
chlorobenzene	112	112		112		112	112	112	112	112
dimethylcyclohexane	112	112		112		112	112	112	112	112
xylene	106	106		106		106	106	106	106	106
benzaldehyde	106	106		106		106	106	106	106	106
ethylbenzene	106	106		106		106	106	106	106	106
xylene-H	105	105		105	105	105	105	105	105	105
benzaldehyde-H	105	105		105	105	105	105	105	105	105
3-methyl-2-furanone	98	98	98	98	98	98	98	98	98	98
methylthiophene	98	98	98	98	98	98	98	98	98	98
furfural		96	96	96	96	96	96	96	96	96
furfural-H		95	95	95	95	95	95	95	95	95
toluene	92	92	92	92		92	92	92	92	92
toluene-H	91	91	91	91	91	91	91	91	91	91
butyrolactone	86	86	86	86	86	86	86	86	86	86
hexene	84	84	84	84	84	84	84	84	84	84
thiophene	84	84	84	84	84	84	84	84	84	84
methylfuran	82	82	82	82	82	82	82	82	82	82
benzene	78	78	78	78	78	78	78	78	78	78
furan	68	68	68	68	68	68	68	68	68	68
sulfur dioxide	64	64	64	64	64	64	64	64	64	64

Table 10. Compounds Most Frequently Reported from Coal Combustion

Compound	Formula	Parent Mass	No. of Cations
acenaphthene	$C_{12}H_{10}$	154	8
acenaphthylene	$C_{12}H_8$	152	6
anthracene	$C_{22}H_{12}$	276	6
benz[a]anthracene	$C_{18}H_{12}$	178	18
benzofluoranthene(s)	$C_{20}H_{12}$	252	7
benzo[ghi]perylene	$C_{24}H_{14}$	302	12
benzo[a]pyrene	$C_{20}H_{12}$	252	23
benzo[e]pyrene	$C_{20}H_{12}$	252	14
biphenyl	$C_{12}H_{10}$	154	7
chrysene	$C_{18}H_{12}$	228	12
coronene	$C_{24}H_{12}$	300	10
dibenzofuran	$C_{12}H_8O$	168	7
dibenzothiophene	$C_{12}H_8S$	184	6
dimethylbenz[a]anthracene	$C_{20}H_{16}$	256	6
fluoranthene	$C_{16}H_{10}$	202	18
fluorene	$C_{13}H_{10}$	166	13
indeno[1,2,3-cd]pyrene	$C_{23}H_{14}$	290	6
methylanthracene(s)	$C_{15}H_{12}$	192	9
methylnaphthalene(s)	$C_{11}H_{10}$	142	7
methylpyrene(s)	$C_{17}H_{12}$	216	9
naphthalene	$C_{10}H_8$	128	11
perylene	$C_{20}H_{12}$	252	12
phenanthrene	$C_{14}H_{10}$	178	18
phenol	C_6H_6O	94	6
pyrene	$C_{16}H_{10}$	202	21
xylene(s)	C_8H_{10}	106	6

Table 10.1. Products Obtained from the Combustion of PVC

Compound	Formula
Benzene	C_6H_6
Toluene	$C_6H_5CH_3$
Xylenes	$C_6H_4(CH_3)_2$
Benzyl chloride	$C_6H_5CH_2Cl$
Chloromethane	CH_3Cl
Chloroethane	C_2H_5Cl
Vinyl chloride	C_2H_3Cl

Tolualdehyde, chlorinated aromatics, HCl, CO and other simple organic compounds.

Table 11. GC/MS Analysis Parameters for the Standards

GC parameters

Injector temperature	180°C		
Initial temperature	150°C		
	Rate (°C/min)	Temperature (°C)	Time (mins)
	5.00	180	3.00
	7.00	250	3.00
	5.00	300	5.00
Split ratio	150		

MS parameters

Detector voltage	1.50 kV
Solvent cut time	2.00
Sampling intervals	0.20
Start mass	20
End mass	350

Table 12. Results from the Combustion of Standard Components for the Purpose of Establishing Detection Limits in the Tubular Furnace

Run 1	Peak identification in solution
Sample:	Standard solution containing 50 mg of naphthalene, fluorene and 2-methyl anthracene
Date:	6/21/95
Results:	Peaks observed for all of the three standards
Run 2	Simulated combustion condition
Sample:	Standard compounds burnt in the furnace tube (50 mg each)
Air flow:	17 mL/min
Date:	6/22/95
Coolant:	water @ 0°C
Results:	Peaks observed for all three standards
Run 3	Detection limits
Sample:	Standard compounds burnt in the tube (30 mg each)
Air flow:	17 mL/min
Date:	6/23/95
Coolant:	water @ 0°C
Results:	Peaks observed for all three standards
Run 4	Decrease sample size
Sample:	Standard compounds burnt in the tube (10 mg each)
Air flow:	17 mL/min
Date:	6/23/95
Coolant:	water @ 0°C
Results:	Peaks observed for all three standards
Run 5	Decrease sample size
Sample:	Standard compounds burnt in the tube (1 mg each)
Air flow:	17 mL/min
Date:	6/26/95
Coolant:	water @ 0°C
Results:	naphthalene, fluorene only were detected, not 2-methylanthracene

Table 13. Results from the Combustion of PVC

Run 1	Analysis of PVC sample
Sample:	10 mg of pure PVC
Air flow:	17 mL/min
Environment:	Room temperature to 400°C
Date:	6/28/95
Coolant:	water
Solvent:	toluene
Results:	Acetone, **benzene**, toluene and solvent impurities
Run 2	Increase sample size
Sample:	50 mg of pure PVC
Air flow:	17 mL/min
Environment:	Room temperature to 400°C
Date:	6/28/95
Coolant:	water
Solvent:	toluene
Results:	**Benzene**, acetone, ethyl benzene, 1,4-dimethyl benzene, **naphthalene**
Run 3	Change coolant
Sample:	50 mg of pure PVC
Air flow:	17 mL/min
Environment:	Room temperature to 700°C
Date:	6/28/95
Coolant:	ice
Solvent:	methylene chloride
Results:	**Benzene**, toluene, ethyl benzene
Run 4	Reanalysis of the above sample using SIM mode
Sample:	50 mg of pure PVC
Air flow:	17 mL/ min
Environment:	Room temperature to 700°C
Date:	6/28/95
Coolant:	ice
Solvent:	methylene chloride
Results:	Methylene chloride and benzene (SIM mode)
Run 5	Change solvent
Sample:	50 mg of pure PVC
Air flow:	17 mL/min
Environment:	Room temperature to700°C
Date:	6/28/95
Coolant:	ice
Solvent:	water
Results:	No peaks could be detected

Table 13 (continued)

Run 6	Reanalysis of above sample using SIM mode
Sample:	50 mg of pure PVC
Air flow:	17 mL/ min
Environment:	Room temperature to 700°C
Date:	6/28/95
Coolant:	ice
Solvent:	water
Results:	No peaks could be detected (SIM mode)

Run 7	
Sample:	50 mg of pure PVC
Air flow:	17 mL/min
Environment:	Room temperature to 700°C
Date:	6/28/95
Coolant:	ice
Solvent:	methylene chloride
Results:	Benzene, toluene, cyclohexane

Run 8	Increase sample size
Sample:	1 g of pure PVC
Air flow:	17 mL/ min
Environment:	Room temperature to 700°C
Date:	6/29/95
Coolant:	ice + $CaCl_2$
Solvent:	methylene chloride
Results:	**Benzene**, cyclohexane, **toluene**, **naphthalene**

Run 9	Change coolant
Sample:	1 g of pure PVC
Air flow:	17 mL/min
Environment:	Room temperature to 700°C
Date:	6/30/95
Coolant:	liquid nitrogen
Solvent:	methylene chloride
Results:	**Benzene**, cyclohexane, **toluene**, ethyl benzene, **naphthalene**, 1,2-dimethyl benzene

Run 10	Analysis of substance condensed in the tube
Sample:	1 g of pure PVC
Air flow:	17 mL/min
Environment:	Room temperature to 700°C
Date:	6/30/95
Coolant:	liquid nitrogen
Solvent:	methylene chloride
Results:	**Benzene, toluene**

Table 13 (continued)

Run 11	Analysis of sample in first trap
Sample:	2 g of PVC
Air flow:	1/2 SCFH of air
Isothermal:	700°C
Date:	7/11/95
Coolant:	ice cold water
Solvent:	2% $NaHCO_3$ over glass beads
Results:	**HCl** and traces of toluene

Run 12	Reanalysis of sample 11 in SIM mode
Sample:	2 g of PVC
Air flow:	1/2 SCFH of air
Isothermal:	700°C
Date:	7/11/95
Coolant:	ice cold water
Solvent:	2 % $NaHCO_3$ over glass beads
Results:	**HCl** (SIM mode)

Run 13	Analysis of second trap
Sample:	2 g of PVC
Air flow:	1/2 SCFH of air
Isothermal:	700°C
Date:	7/11/95
Coolant:	ice
Solvent:	methylene chloride
Results:	**Benzene, toluene, styrene**

Table 14. Results from the Combustion of Coal in the Furnace

Run 1	
Sample:	2 g of coal
Air flow:	17 mL/min
Isothermal:	800°C
Date:	7/2/95
Coolant:	liquid nitrogen
Solvent:	methylene chloride
Results:	Benzene, cyclohexane, toluene, **phenol, 4-methyl phenol**, decane, undecane
Note:	There was tar formation observed and hence the air flow was increased to 470 ml/min.
Run 2	Increase flow rate
Sample:	2 g of coal
Air flow:	1 SCFH (approximately 470 ml/min) of air
Isothermal:	800°C
Date:	7/5/95
Coolant:	liquid nitrogen
Solvent:	methylene chloride
Results:	Benzene, heptane, methyl benzene, 1-chlorohexane, octane, 2-methyl octane, ortho/para xylene, nonane, **phenol,** 1,2,3-trimethylphenol, decane, **o-cresol,** cyclopentane derivative, **phenenthrene,** isopropyl myristate, oxirane
Run 3	Change coolant
Sample:	5 g of coal
Air flow:	1 SCFH of air
Isothermal:	800°C
Date:	7/11/95
Coolant:	ice
Solvent:	methylene chloride
Results:	Cyclohexane, 1-heptane, methyl cyclohexane, octane, octene, trimethyl cyclohexane, o-xylene, nonane, **phenol**, cyclopropane, 1,2,3- trimethyl benzene, decane, dodecane, **o-cresol, 2,5-dimethyl phenol, naphthalene**

Table 14 (continued)

Run 4	Reduce flow rate
Sample:	2 g of coal
Air flow:	1/2 SCFH of air
Isothermal:	800°C
Date:	7/18/95
Coolant:	ice
Solvent:	methylene chloride
Results:	Toluene, 1,3-dimethyl cyclohexane, butyl acetate, octane, 1,2-dimethyl cyclohexane, 2,6-dimethyl heptane, 1,3,5-trimethyl cyclohexane,1-chlorooctane, 2-methyl octane, 1,2,3-trimethyl cyclohexane,1,2-dimethyl benzene, 3-methyl octane, 1-ethyl-4-methyl cyclohexane, nonane, 3-methyl cyclopentane, 3-ethyl-2-methyl heptane, propyl benzene, **phenol**, 2-methyl nonane, 1,2,3-trimethylbenzene, decane, **o-cresol**, decane derivatives, **naphthalene**, dodecane, hexadecane

Run 5	Sample from run 4 concentrated
Sample:	2 g of coal
Air flow:	1/2 SCFH of air
Isothermal:	800°C
Date:	7/18/95
Coolant:	ice
Solvent:	methylene chloride
Results:	Toluene, 3-methyl thiophene, 2-octene, octane, 1,1,2-trimethyl cyclohexane, 2-methyl octane , 1,2-dimethyl benzene, nonane, 3-methyl nonane, **phenol**, decane, ethyl methyl benzene, decane, **2-methyl phenol**, tetradecane, undecane, **naphthalene**, tridecane, tratetracontane, 2-methyl decane

Note 1. The compounds underlined are those which occur in almost every analysis done on the coal sample. The compounds in bold are those which were identified by literature searches as being the most common.

Note 2. Runs 4 and 5 were analyzed after the solvent was concentrated to 1 mL from about 25 mL. The ease of detection and identification increases when the samples are concentrated.

Note 3. All the peaks so far have been tentatively identified.

Table 15. GC/MS Analysis Parameters for Coal

GC parameters

Injector temperature	150°C		
Initial temperature	100°C		
	Rate (°C/min)	Temperature (°C)	Time (mins)
	5.00	150	2.00
	5.00	200	2.00
	5.00	250	2.15
Split ratio	150		

MS parameters

Detector voltage	1.50 kV
Solvent cut time	4.00
Sampling intervals	0.75
Start mass	40
End mass	350

Table 16. Standard Procedure for GC/MS Identifications

1. Run a control on a solvent control sample. This needs to be done to demonstrate that any peak obtained can be compared against a solvent blank to verify it's origin.

2. Each sample should be analyzed at least twice. This avoids errors which may occur due to possible contamination of the capillary column.

3. In case of the library search using the software program, the peak listed first may not necessarily be the true identity of the compound. Look at all the choices listed (within reasonable similarity index).

4. On finding a peak of significance, the peak must be identified by the GC/MS analysis of a standard (a solution of the tentatively identified compound). The standard should be analyzed on an identical program. If the retention times are identical, identification is positive.

Figure 1. DTG curves for coal 92073 at slow (10°C/min) and fast (100°C/min) heating rates.

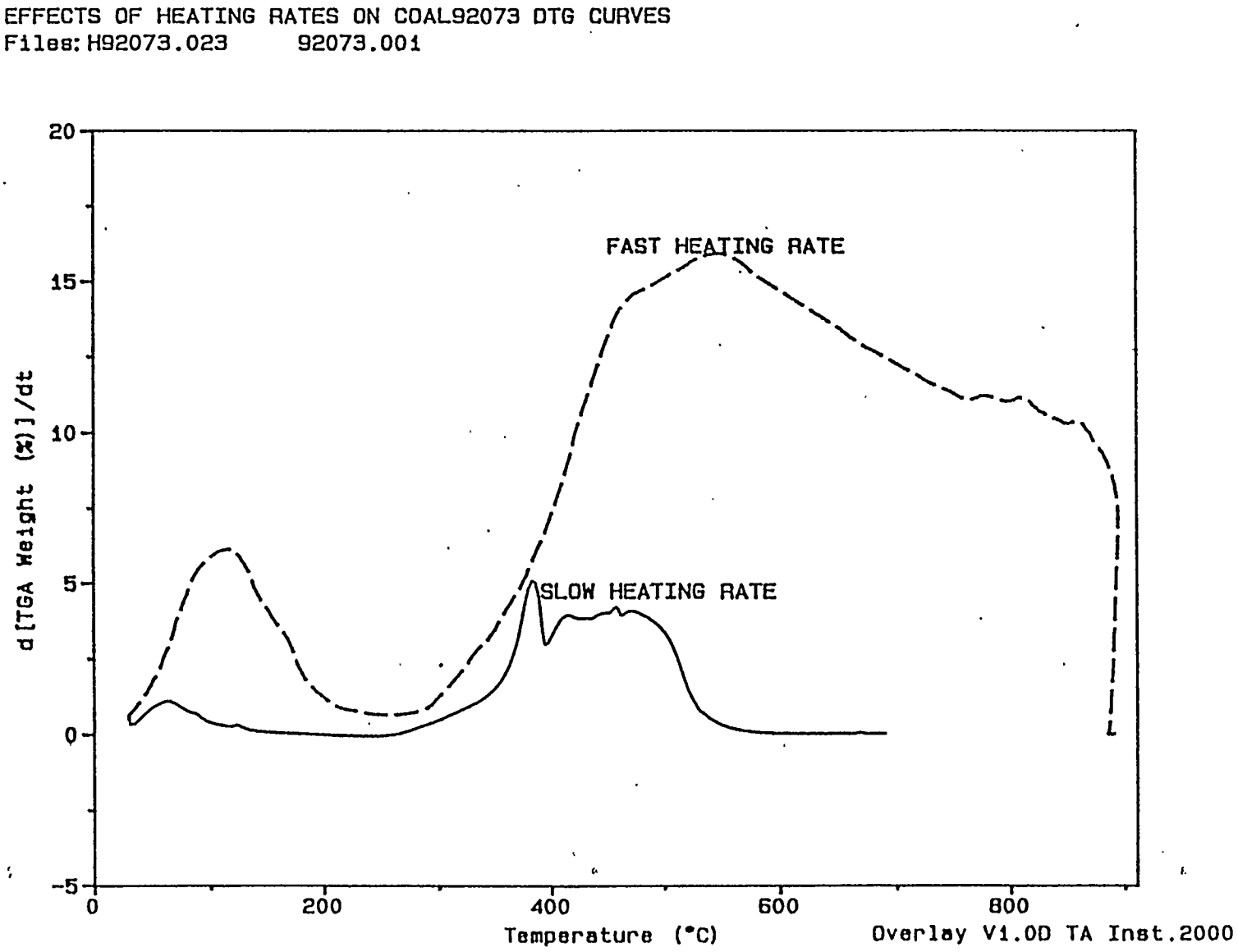

Figure 2. DTG curves for PVC at slow (10°C/min) and fast (100°C/min) heating rates.

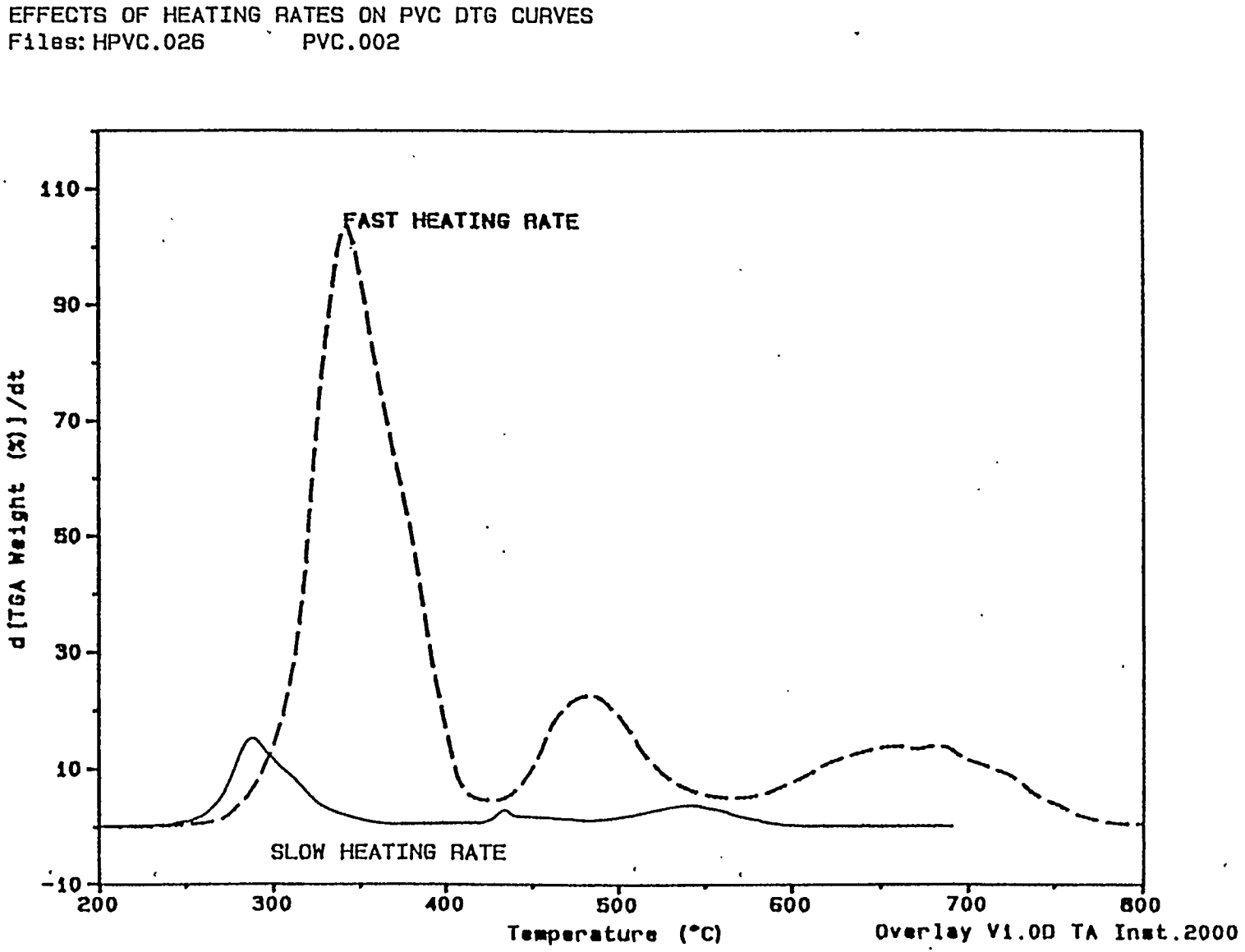

Figure 3. TG curves for blend 035122 and its components; coal 90003, PVC, cellulose, and newspaper.

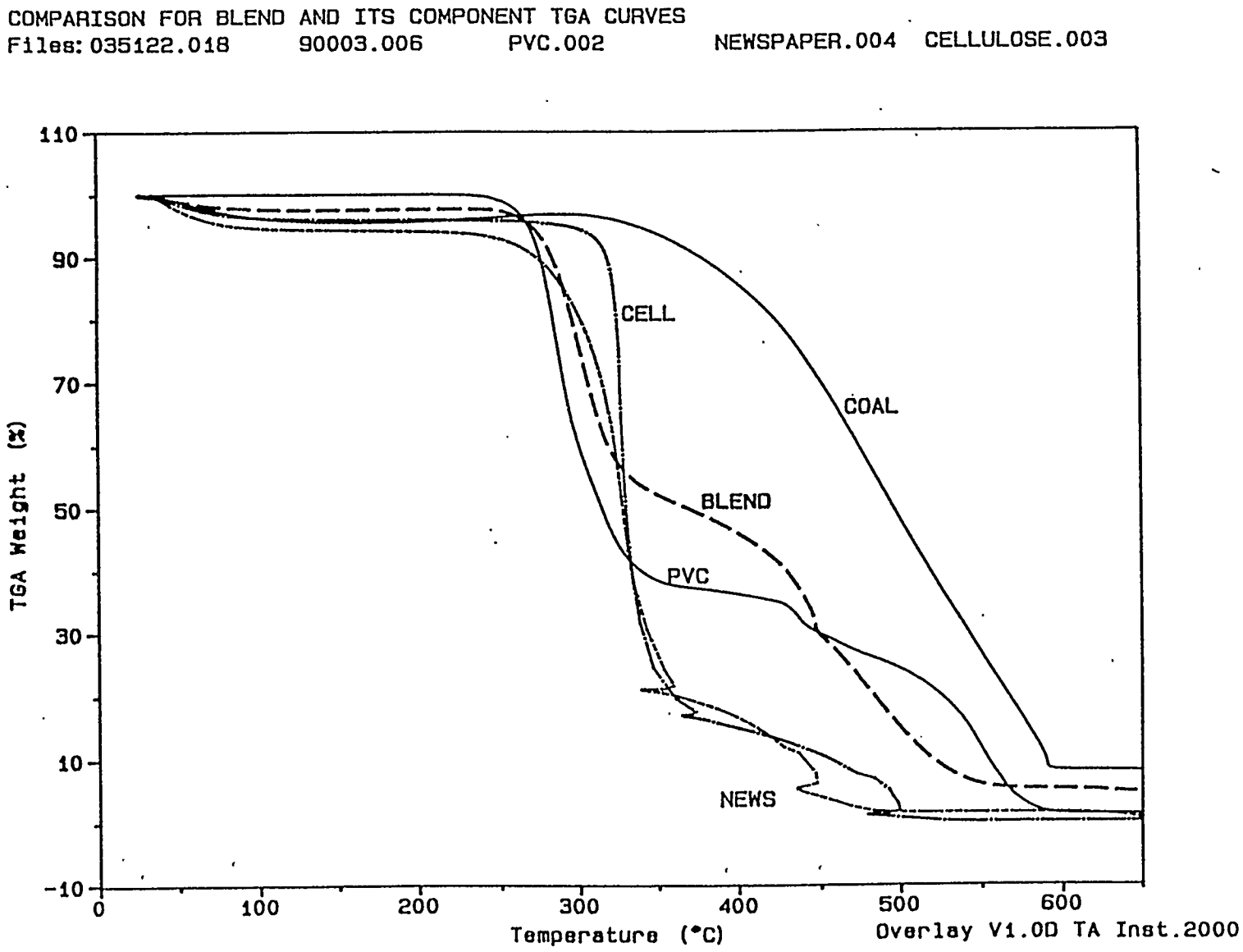

Figure 4. TG curves for blend 035122 and its components; coal 90003, PVC, cellulose, and newspaper.

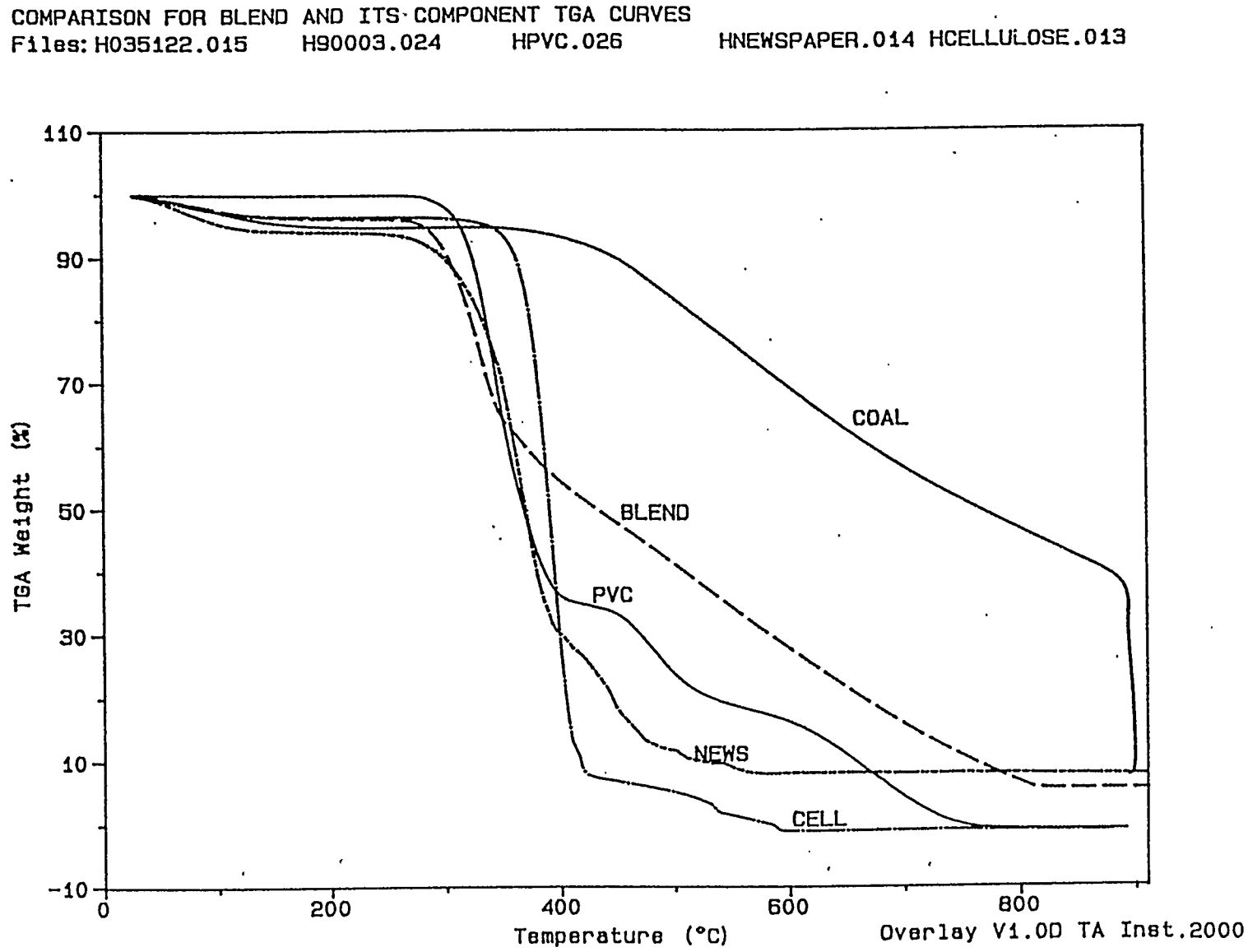

Figure 5. TG curves for blend 735122 and its components; coal 92073, PVC, cellulose, and newspaper.

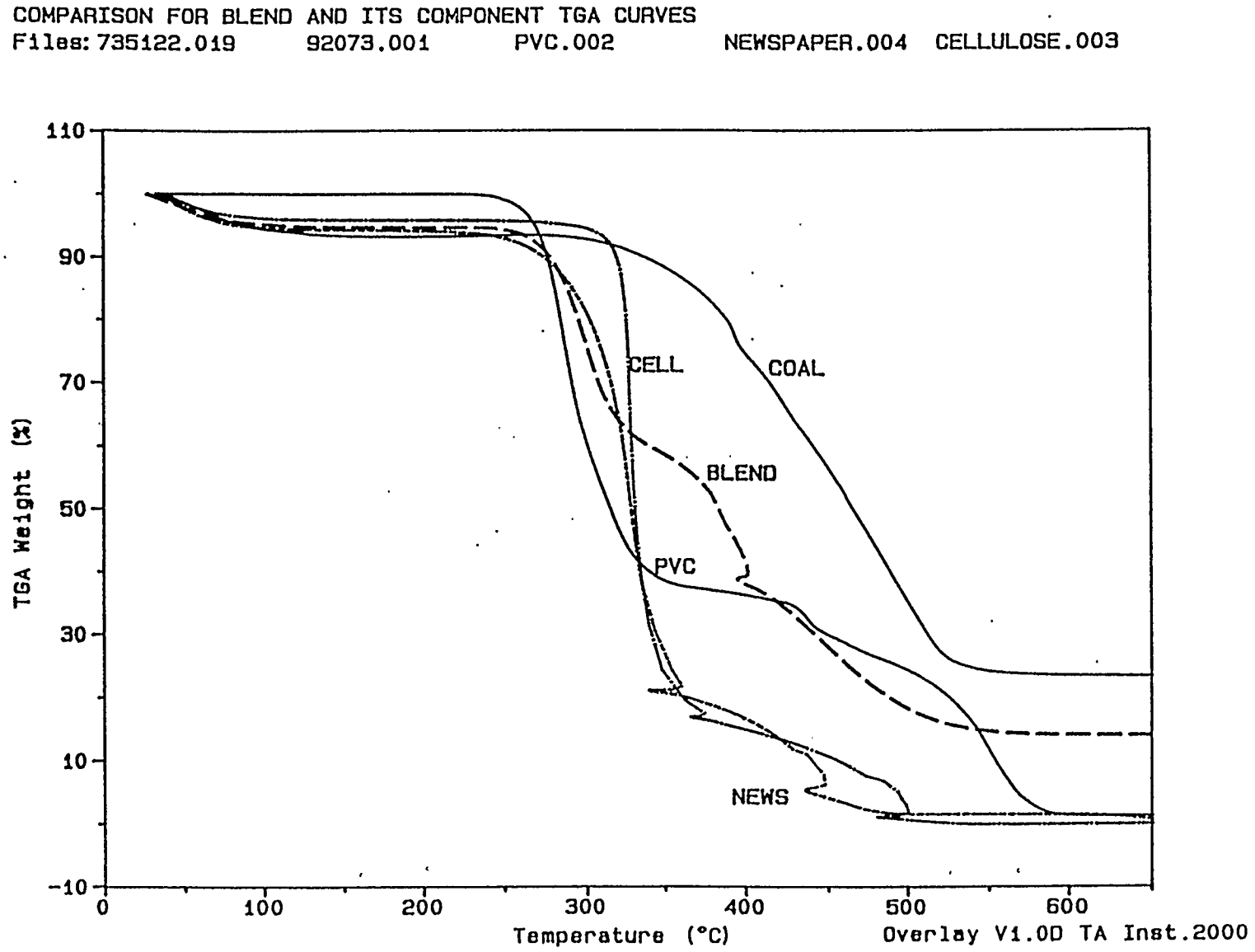

Figure 6. TG curves for blend 735122 and its components; coal 92073, PVC, cellulose, and newspaper.

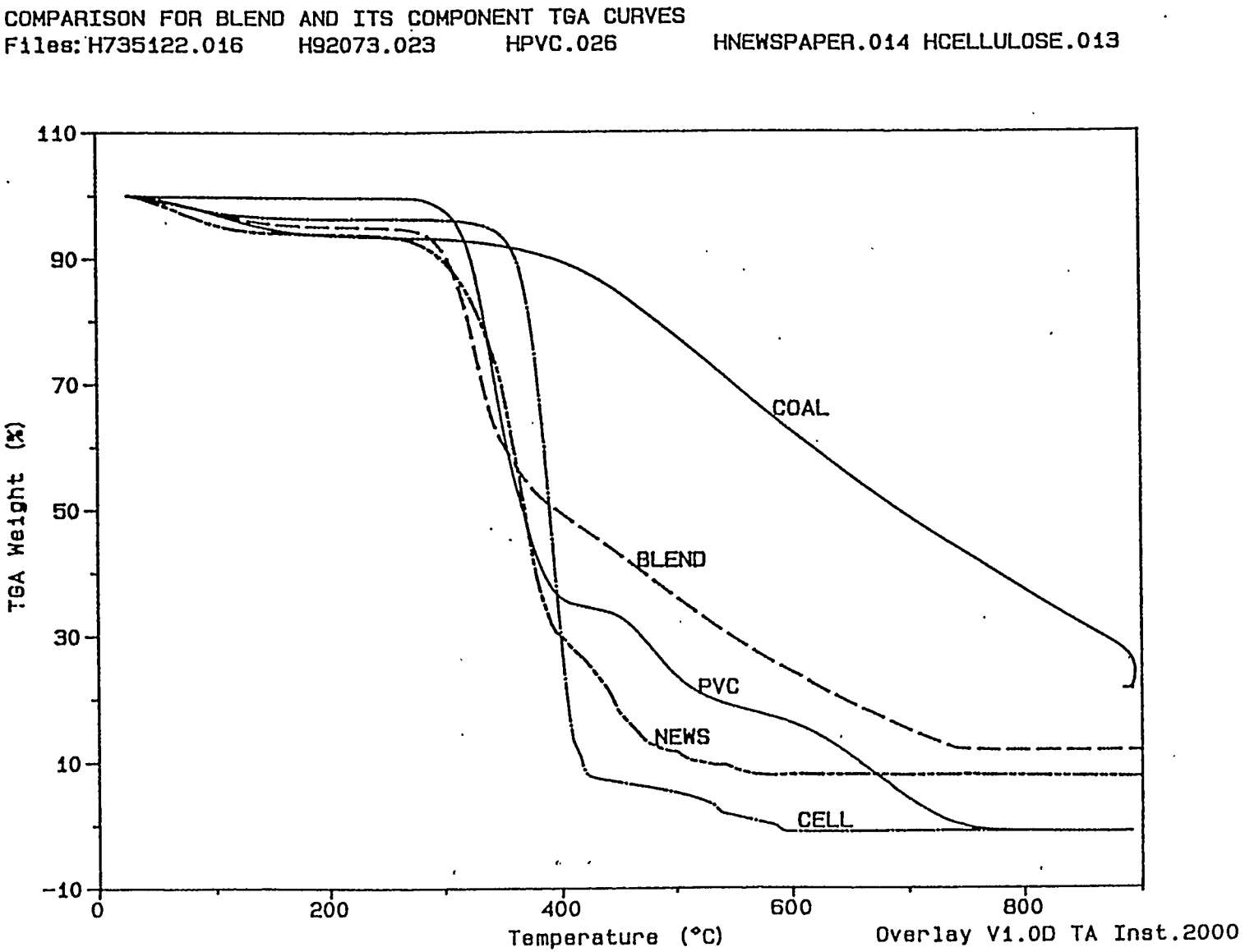

Figure 7. TG curves for coals 95010, 95011, 95031, 92073, and 90003 at the slow heating rate.

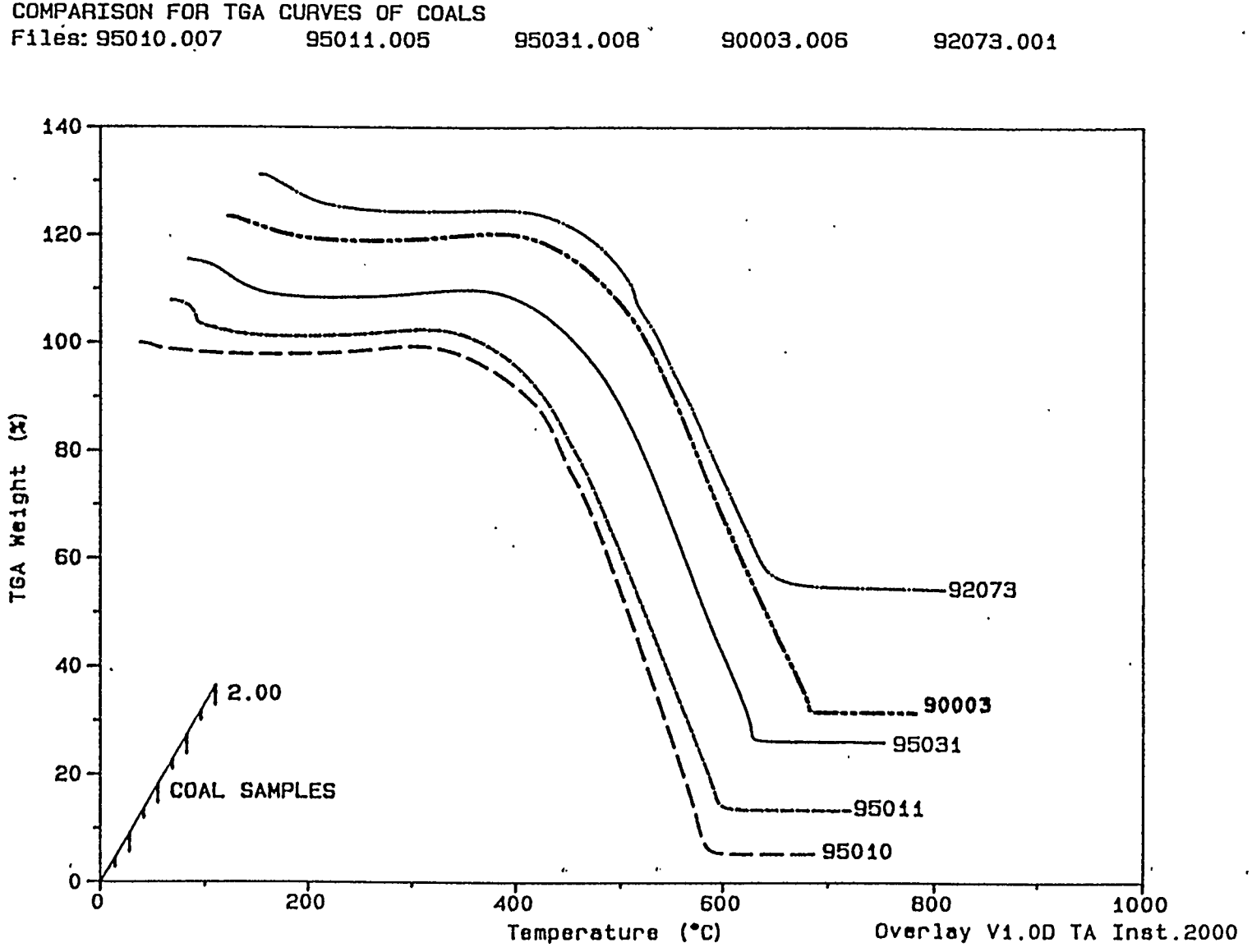

Figure 8. Three-dimensional FTIR spectra of combustion products of PVC at the fast heating rate.

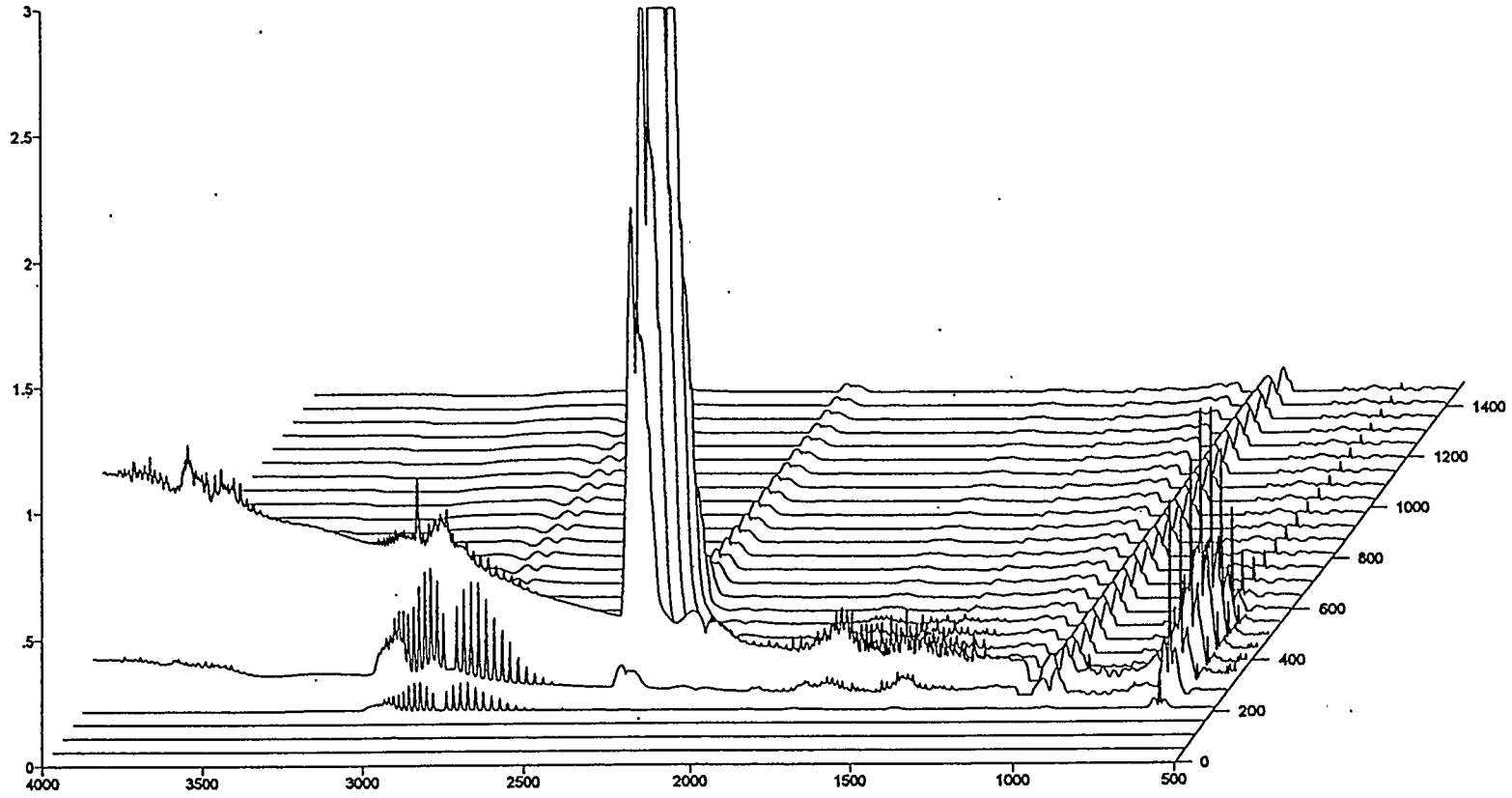

Figure 9. Three-dimensional FTIR spectra of combustion products of newspaper at the fast heating rate.

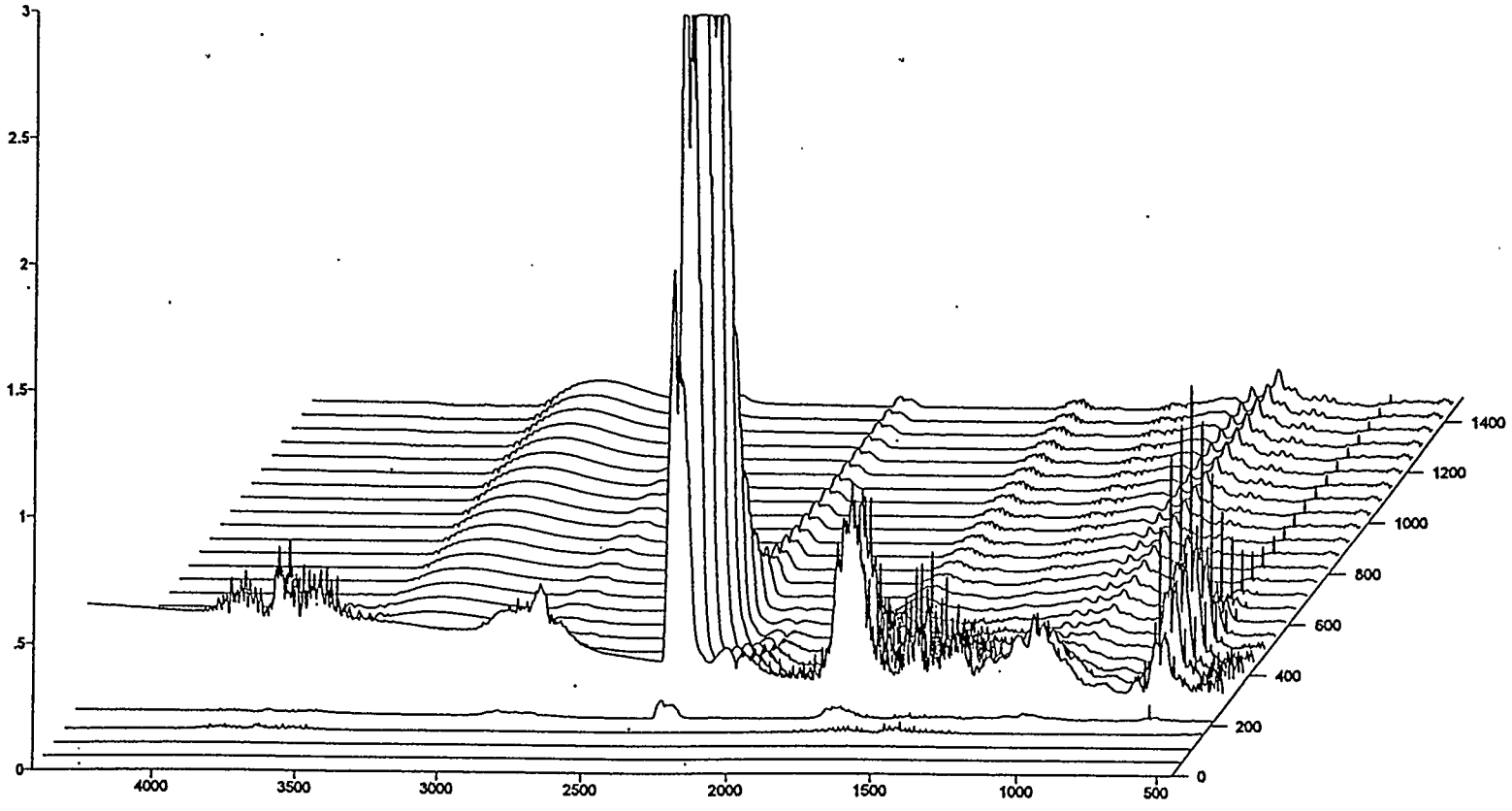

Figure 10. Three-dimensional FTIR spectra of combustion products of coal 92073 at the fast heating rate.

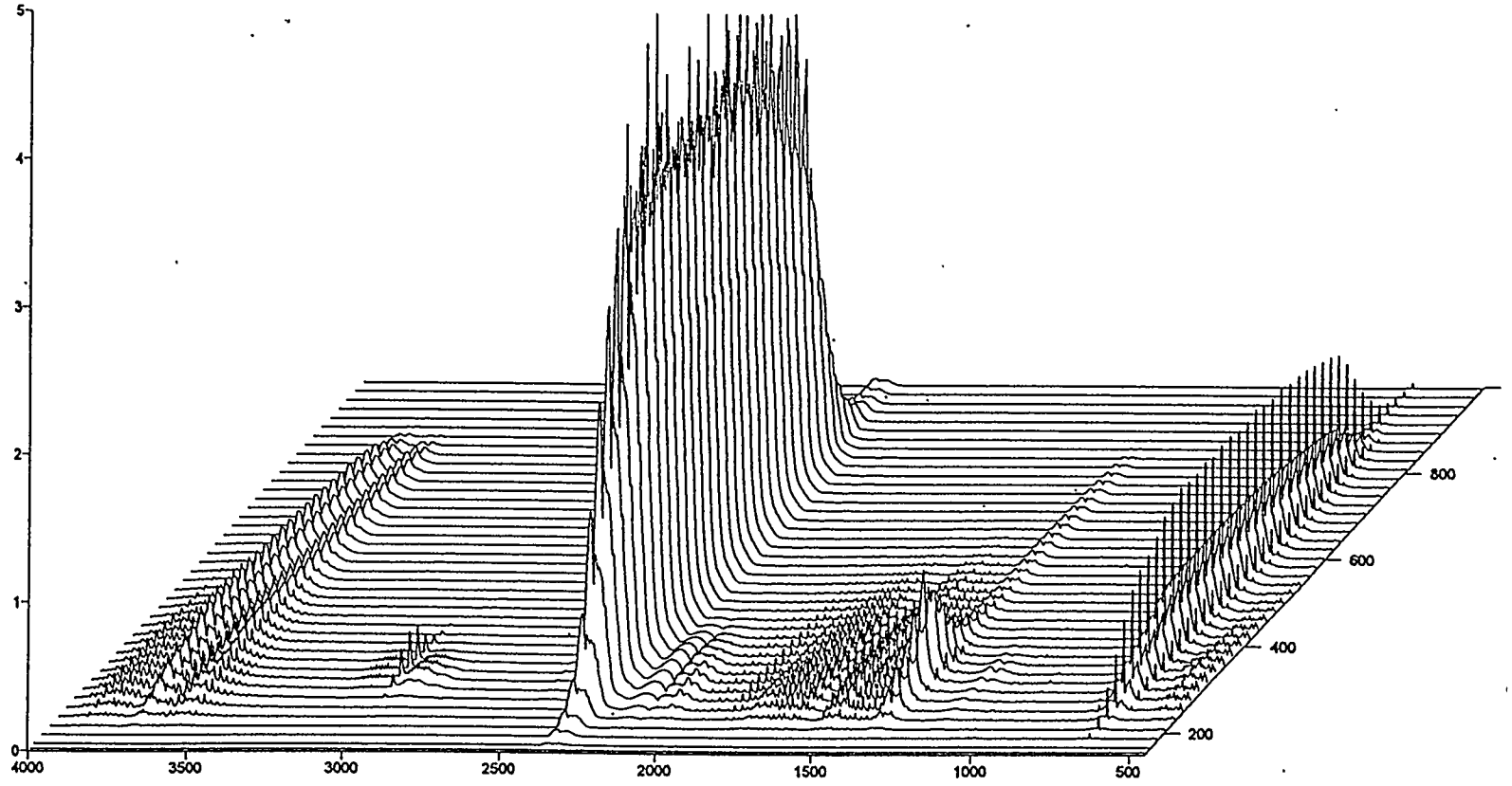

Figure 11. Three-dimensional FTIR spectra of combustion products of blend 735122 at the fast heating rate.

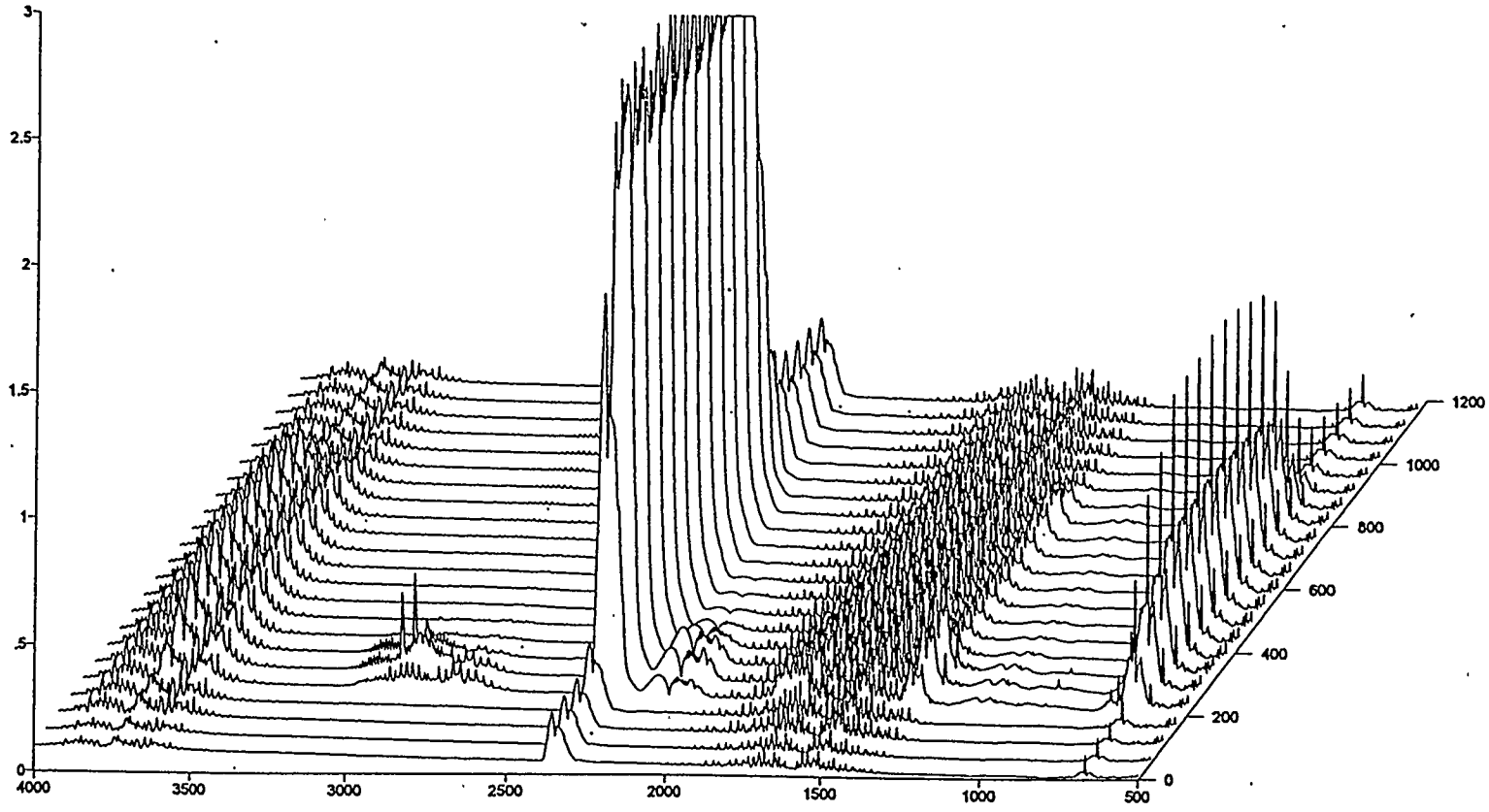

Figure 12. Three-dimensional FTIR spectra of combustion products from coal 95010 at the slow heating rate.

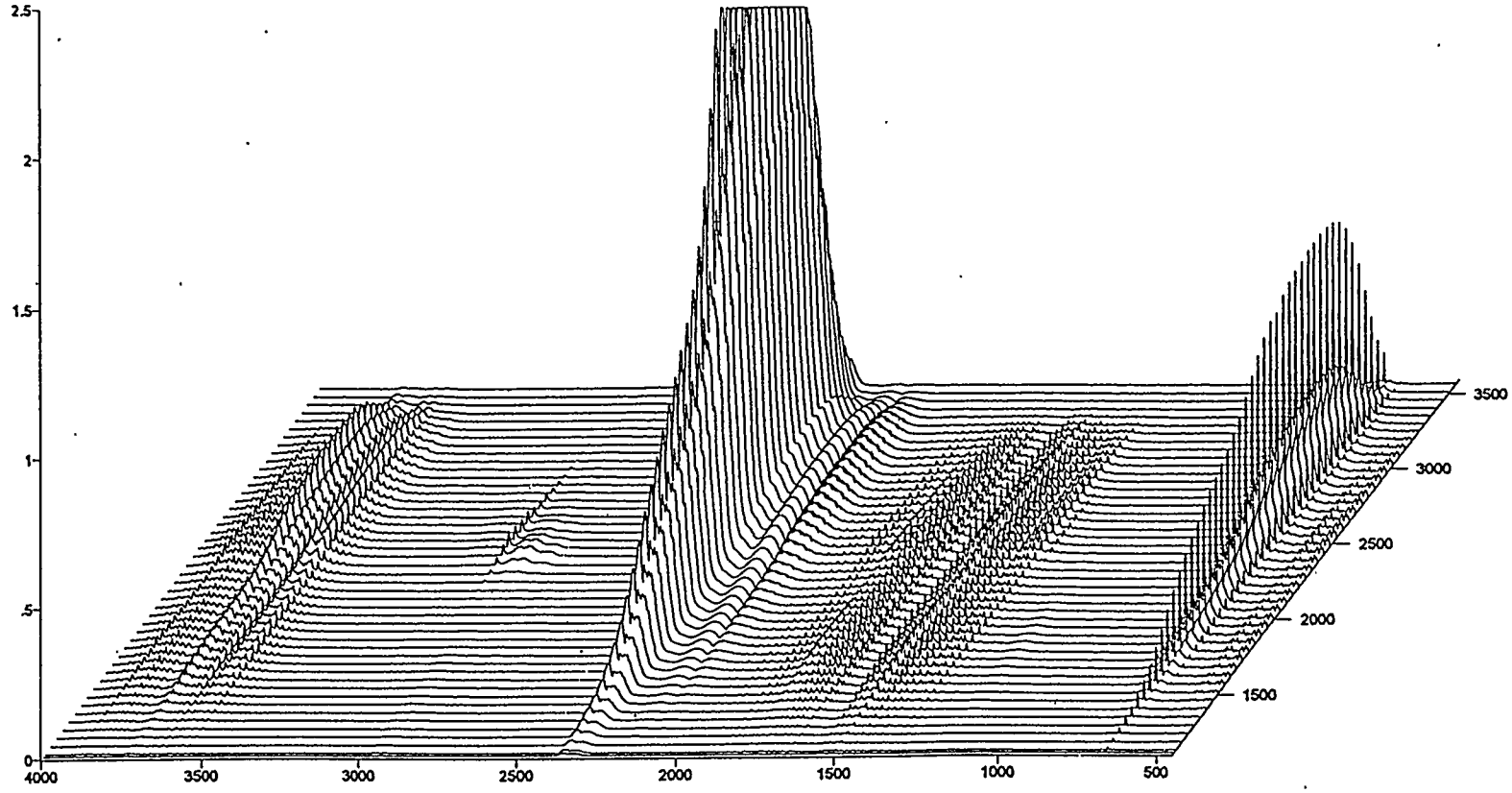

Figure 13. Three-dimensional FTIR spectra of combustion products from coal 95011 at the slow heating rate.

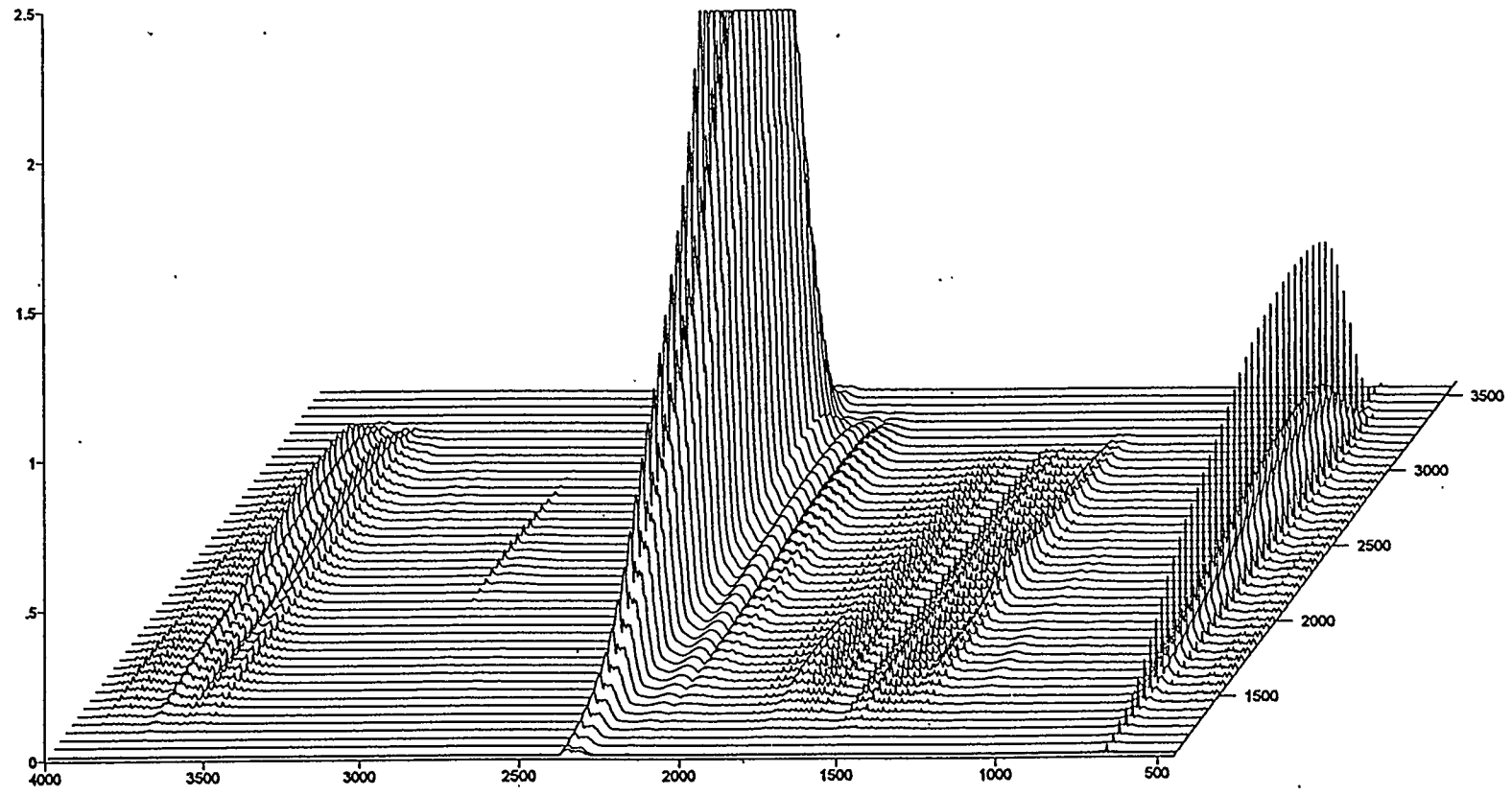

Figure 14. Three-dimensional FTIR spectra of combustion products from coal 95031 at the slow heating rate.

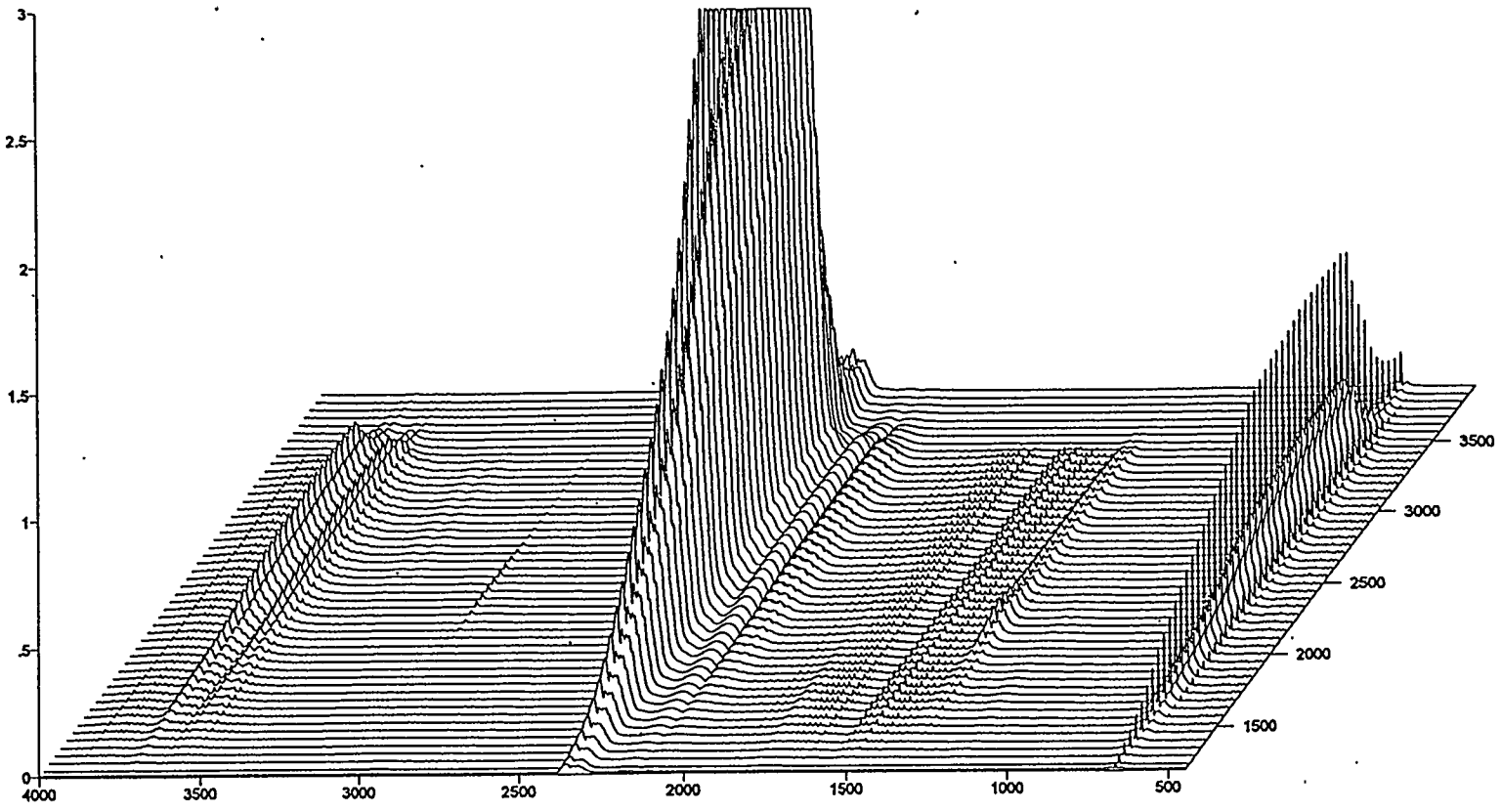

Figure 15. Three-dimensional FTIR spectra of combustion products of blends of 95010 at the slow heating rate.

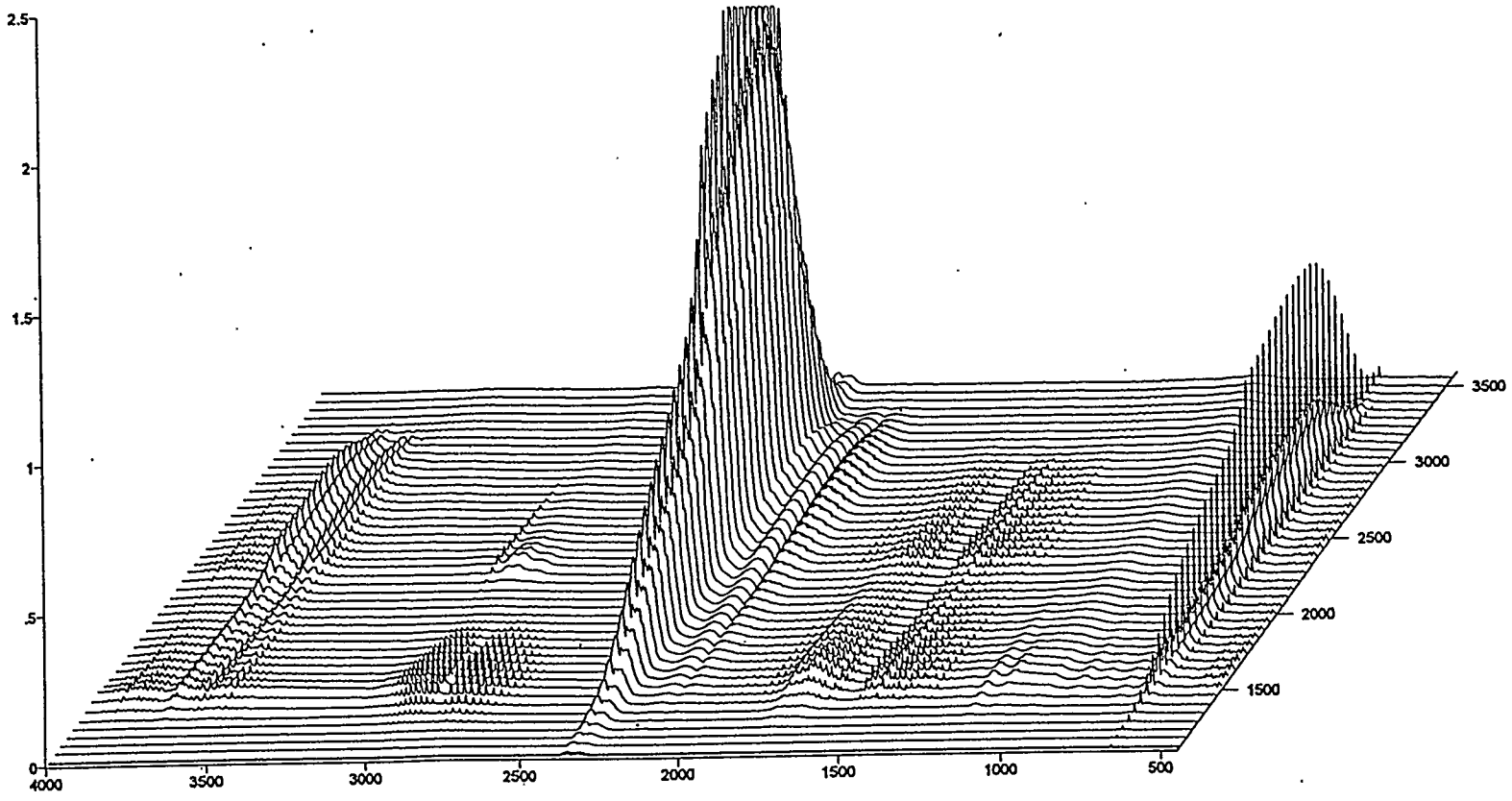

Figure 16. Three-dimensional FTIR spectra of combustion products of blends of 95011 at the slow heating rate.

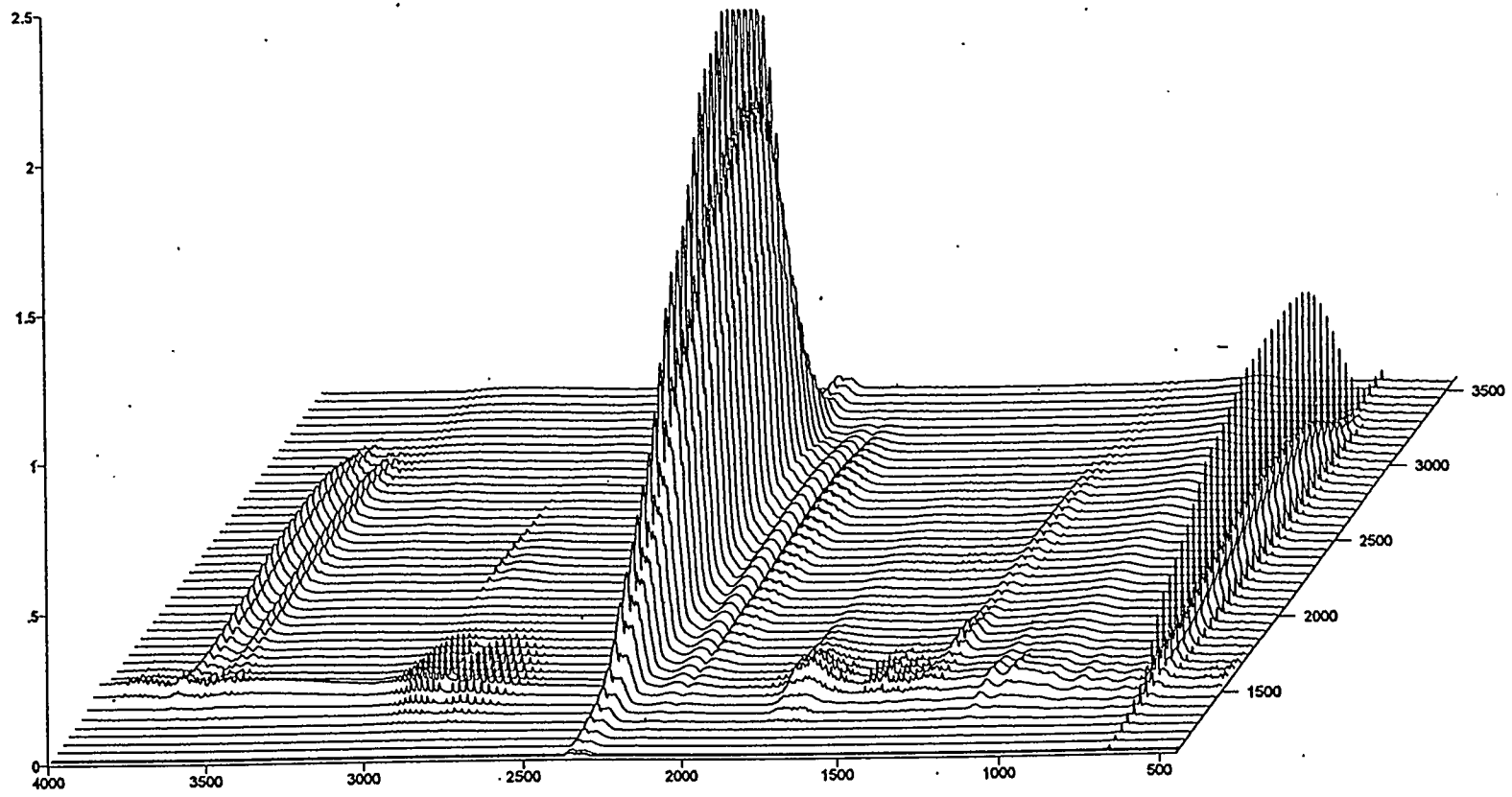

Figure 17. Three-dimensional FTIR spectra of combustion products of blends of 95031 at the slow heating rate.

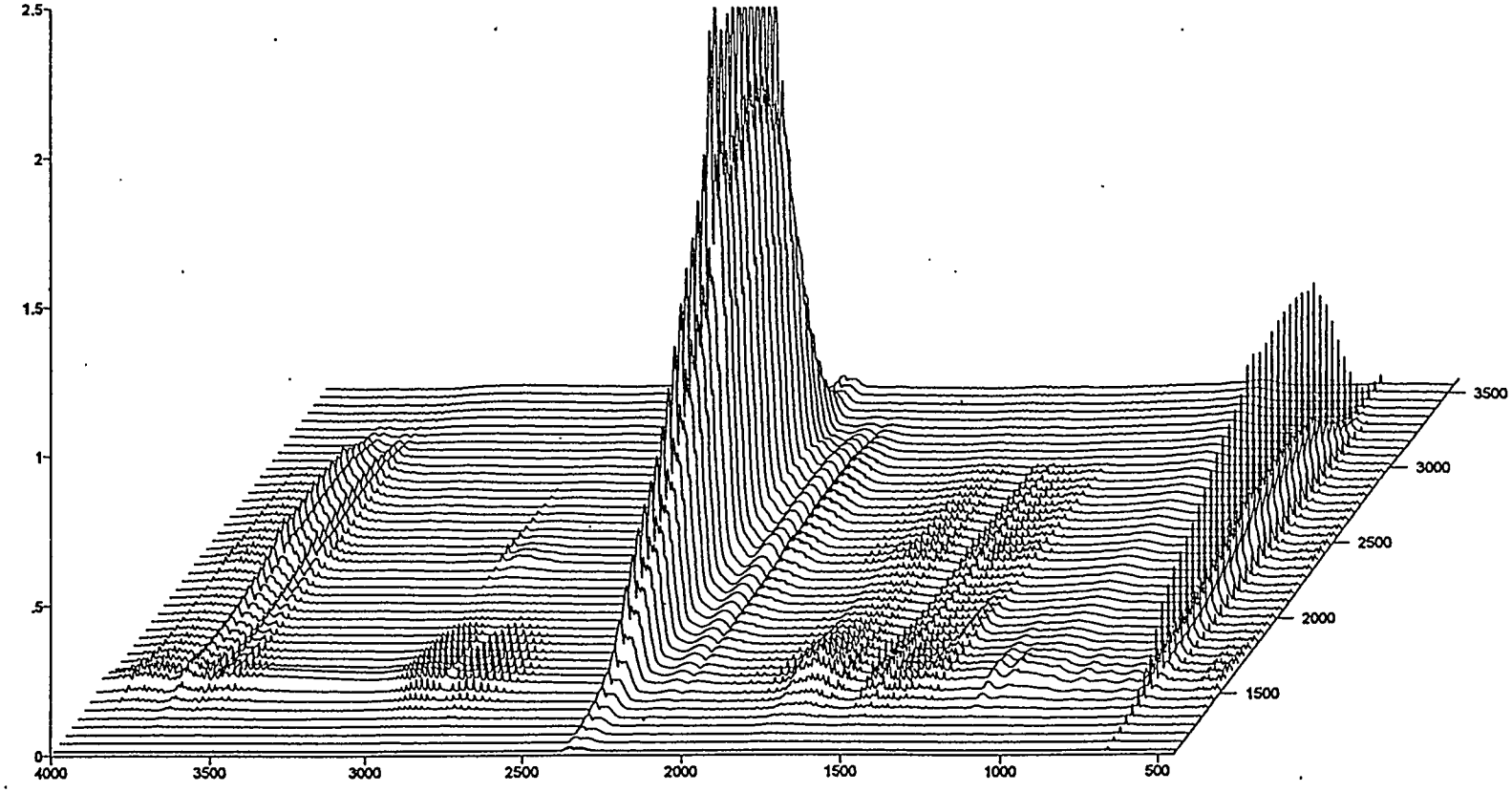

Figure 18. Three-dimensional FTIR spectra of combustion products of blends of 95010 at the fast heating rate.

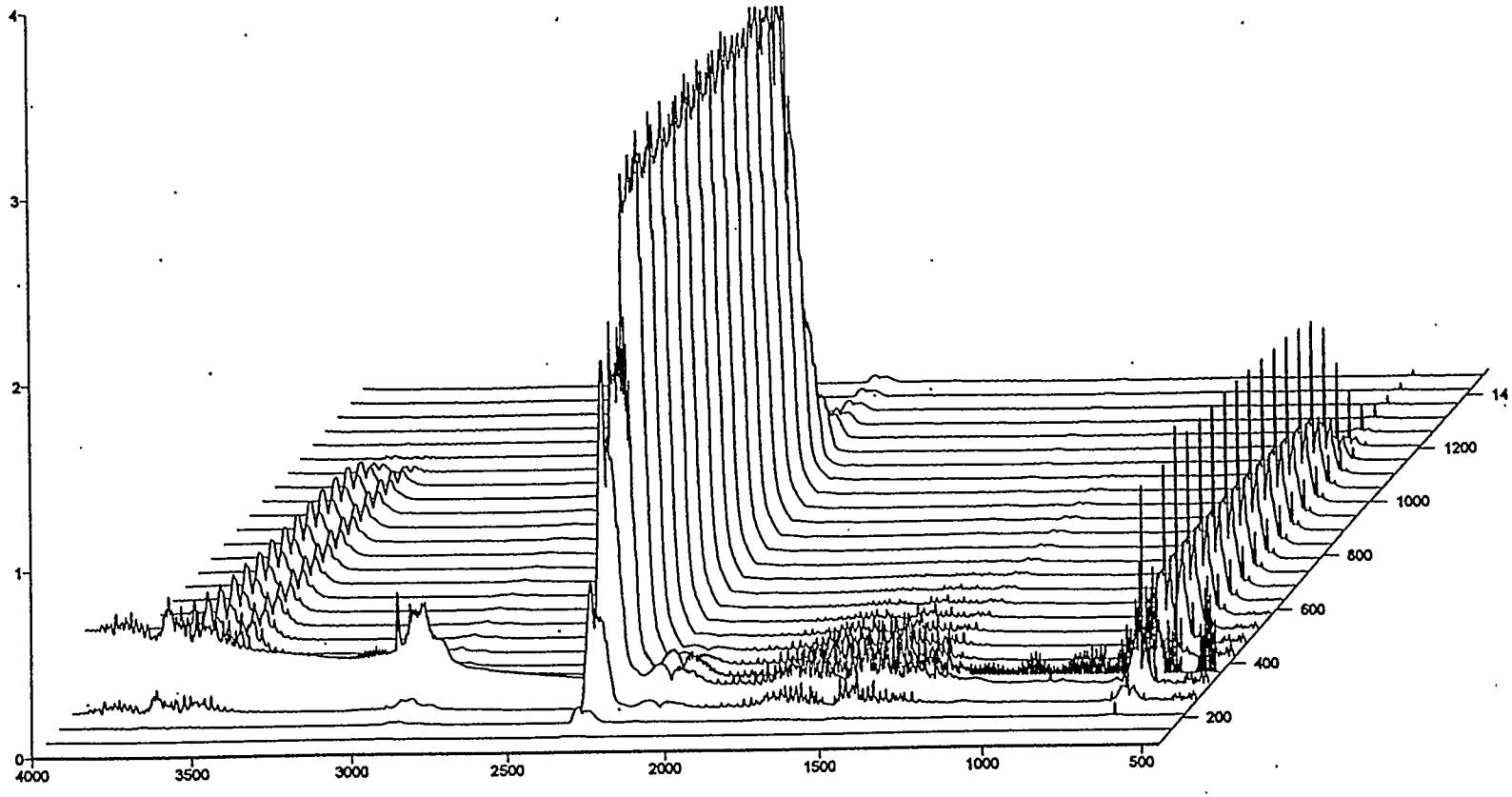

Figure 19. Three-dimensional FTIR spectra of combustion products of blends of 95011 at the fast heating rate.

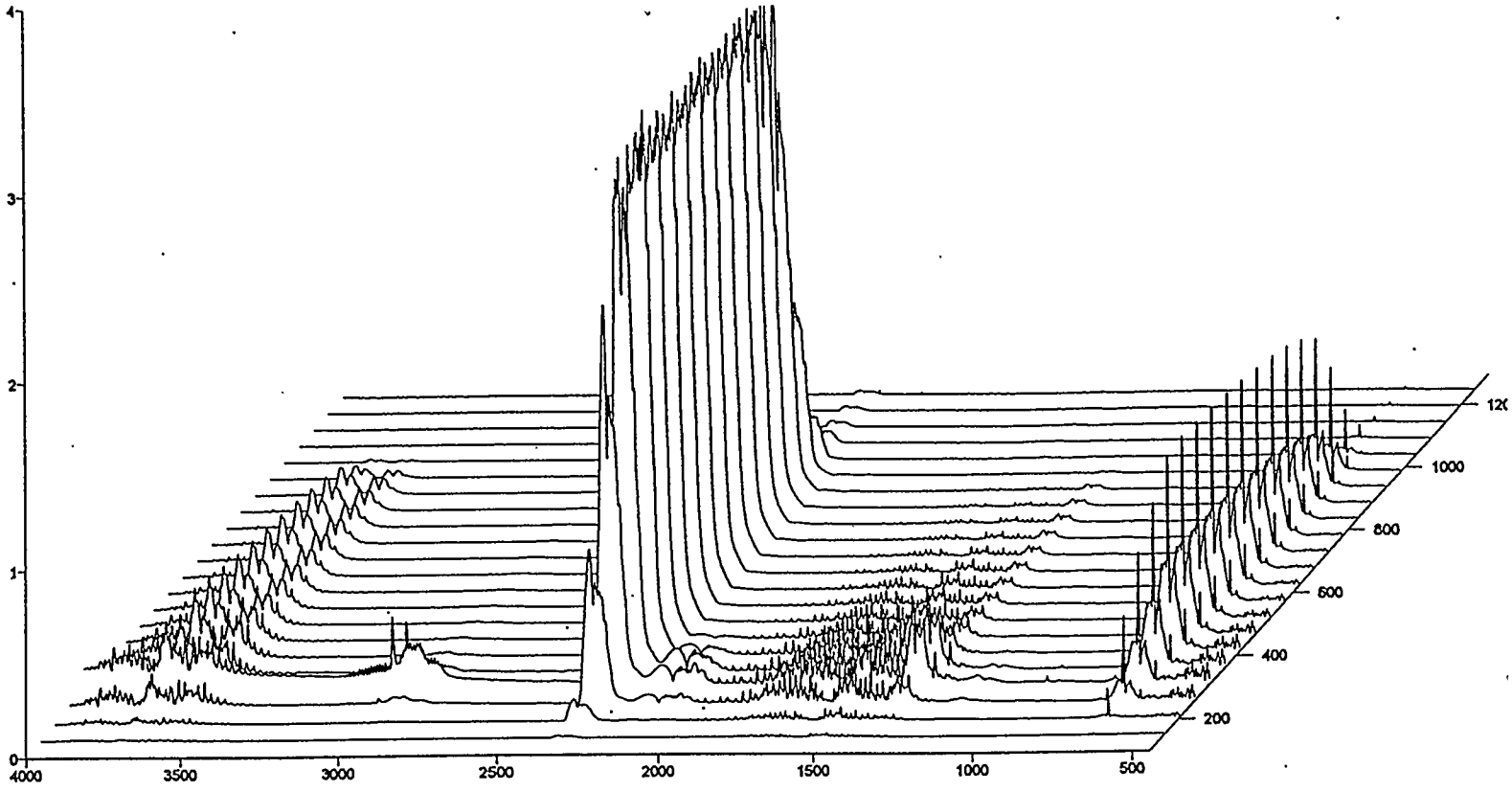

Figure 20. Three-dimensional FTIR spectra of combustion products of blends of 95031 at the slow heating rate.

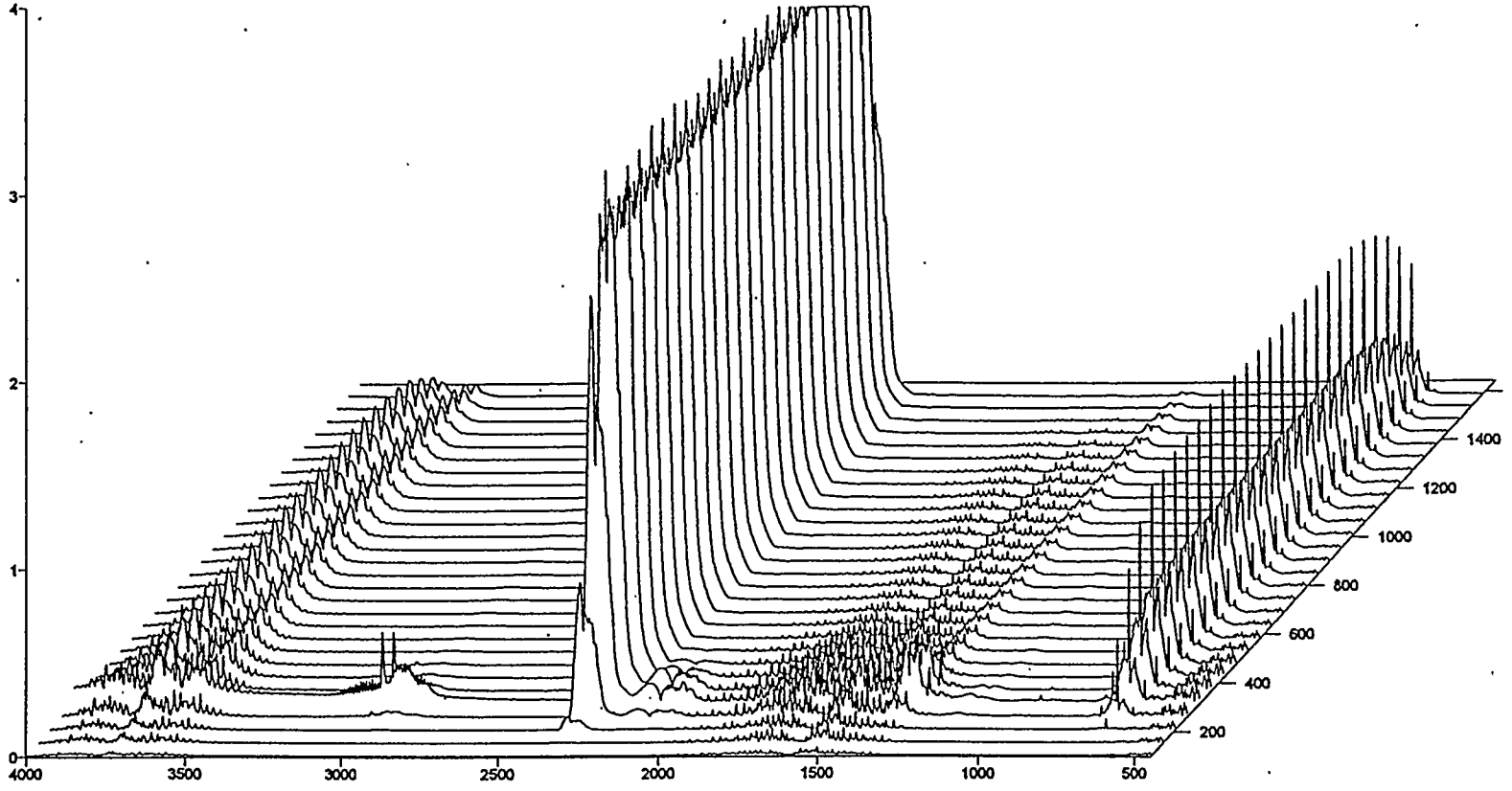

Figure 21. Three-dimensional FTIR spectra of combustion products from mixtures of coal 95010 with newspaper and PVC at the fast heating rate.

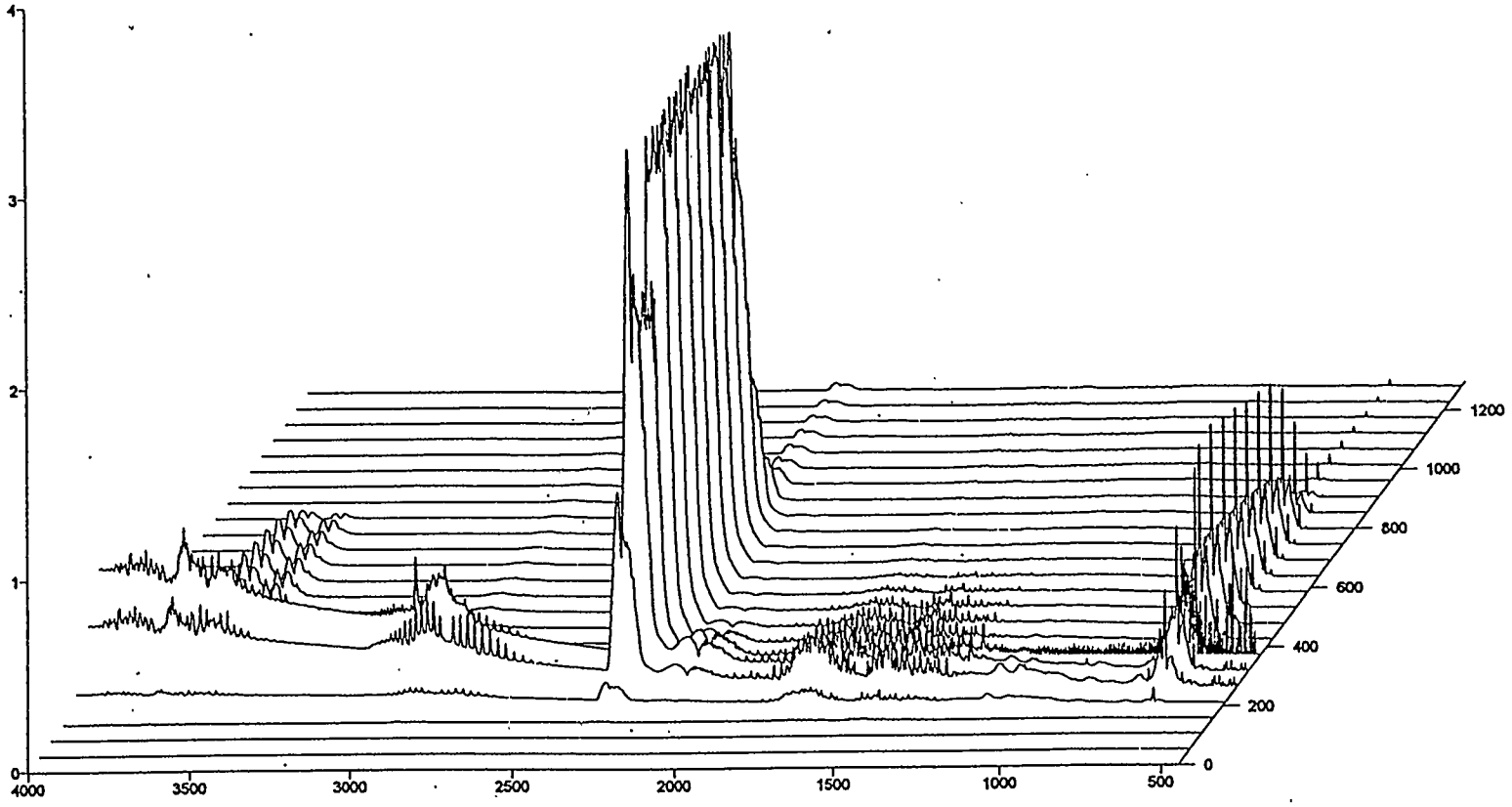

Figure 22. Three-dimensional FTIR spectra of combustion products from mixtures of coal 95011 with newspaper and PVC at the fast heating rate.

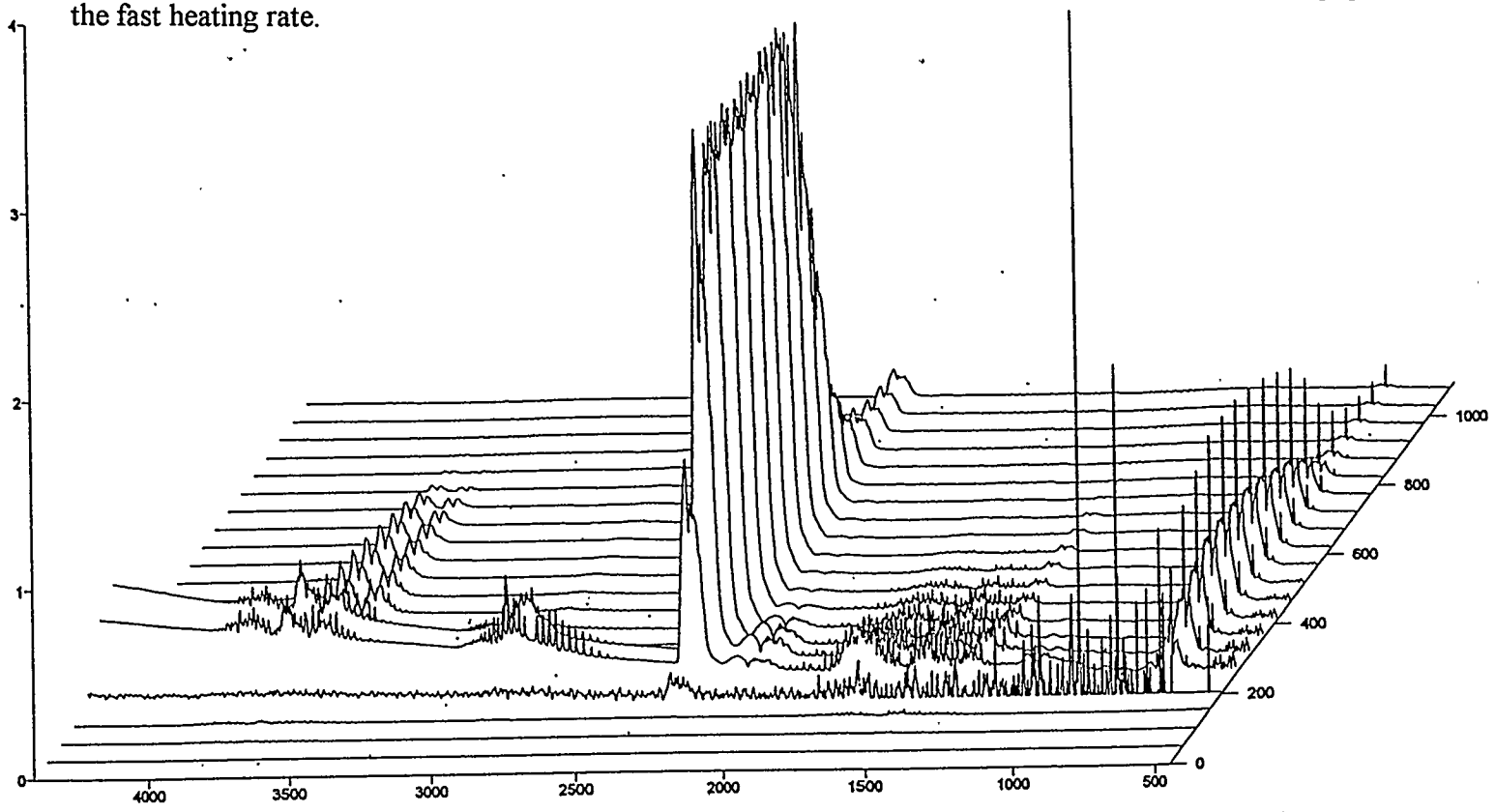

Figure 23. Three-dimensional FTIR spectra of combustion products from mixtures of coal 95031 with newspaper and PVC at the fast heating rate.

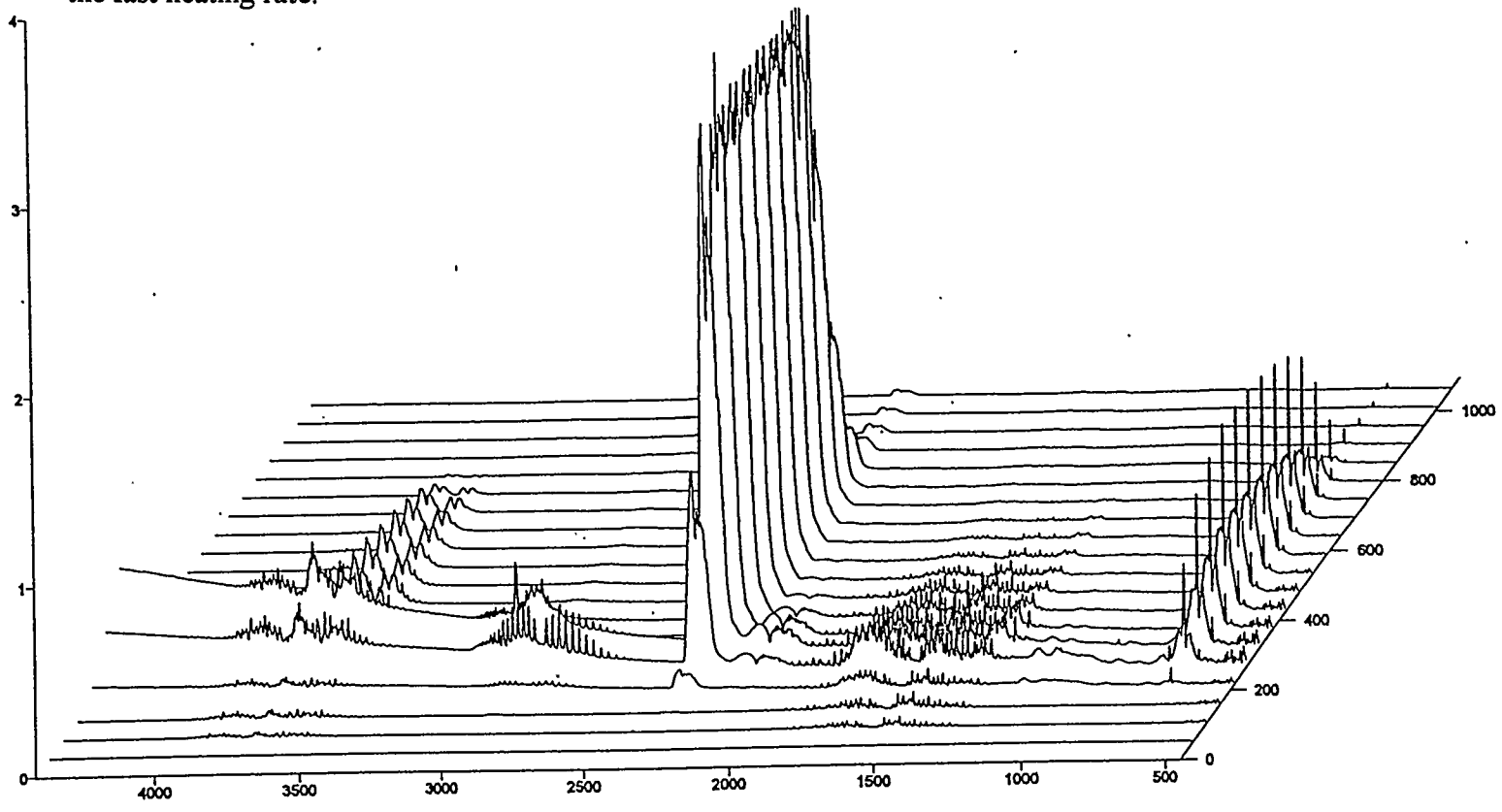

Figure 24. Profiles of some major peaks for combustion products of PVC at the slow heating rate.

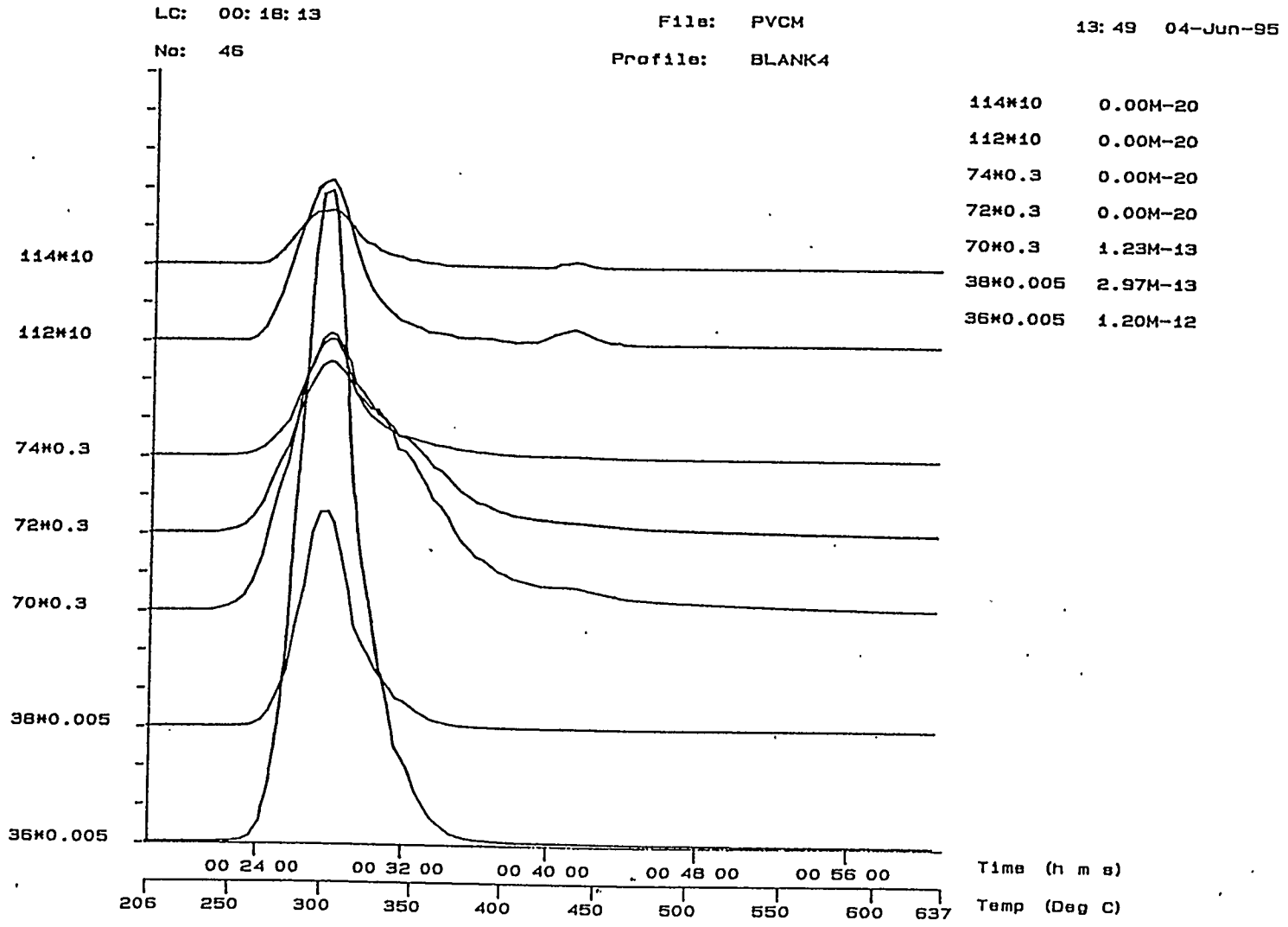

Figure 25. Profiles of some major peaks for combustion products of PVC at the slow heating rate.

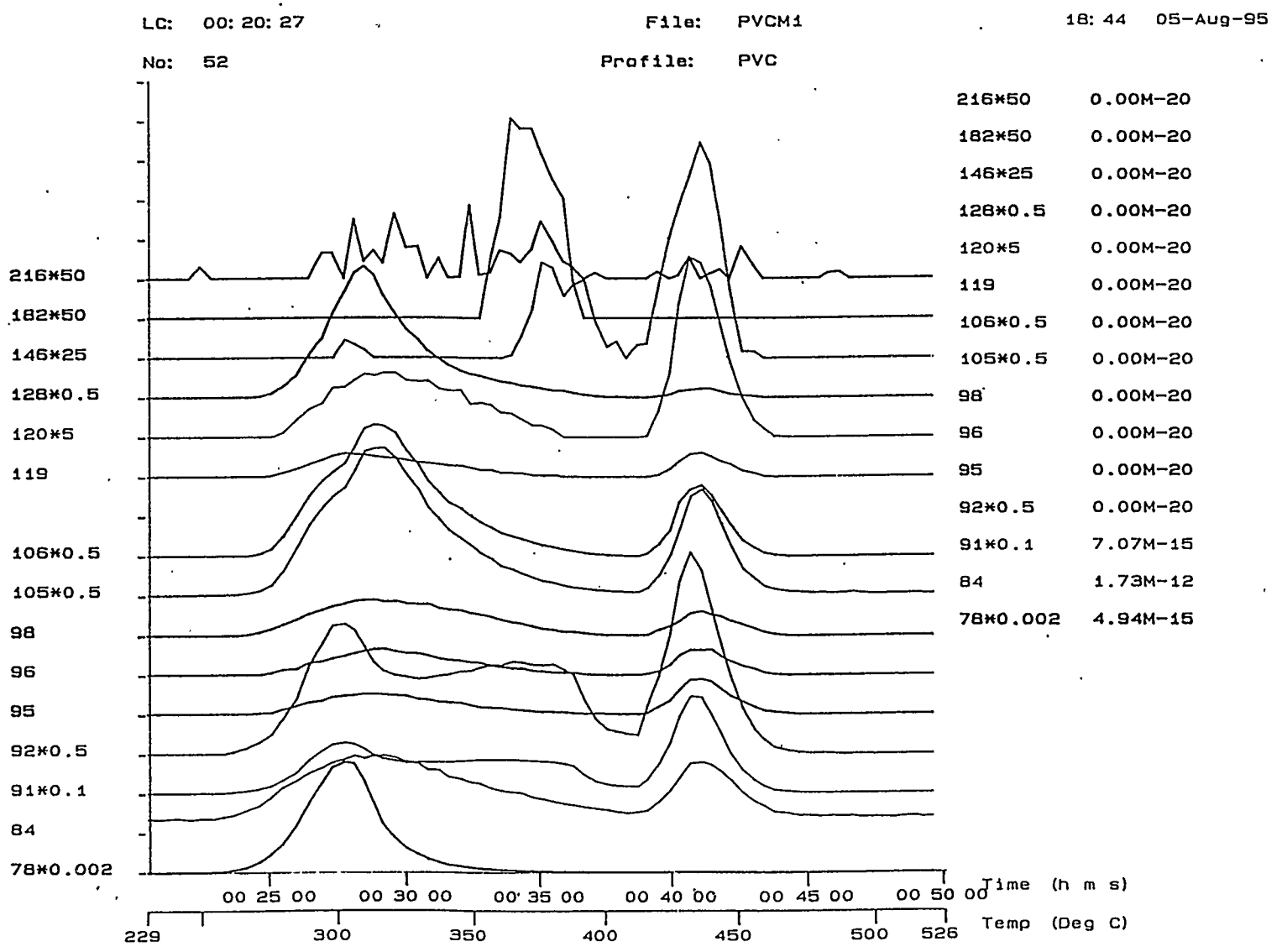

Figure 26. Profiles of some major peaks for combustion products of PVC at the slow heating rate.

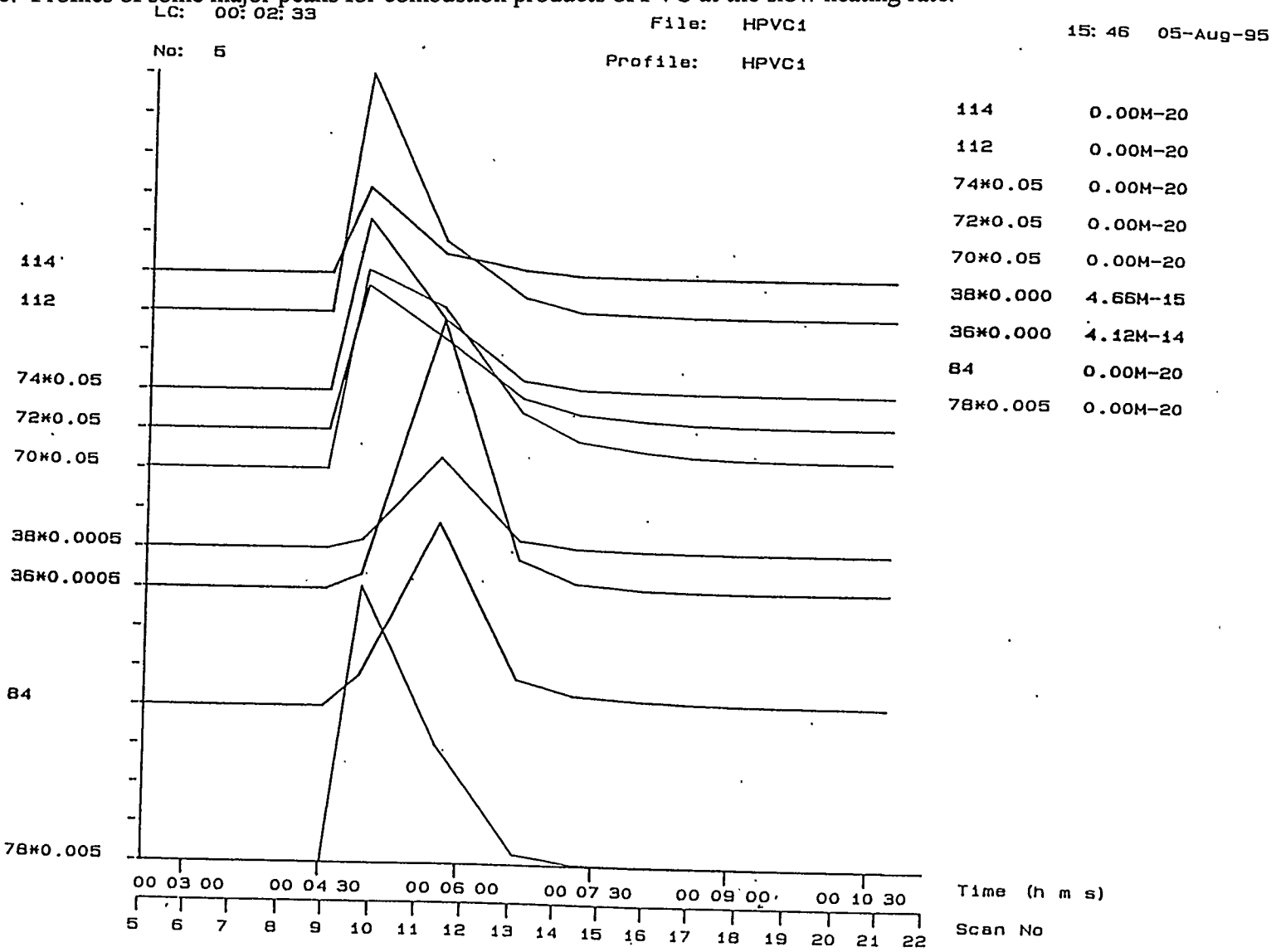

Figure 27. Profiles of some major peaks for combustion products of coal 92073 at the fast heating rate.

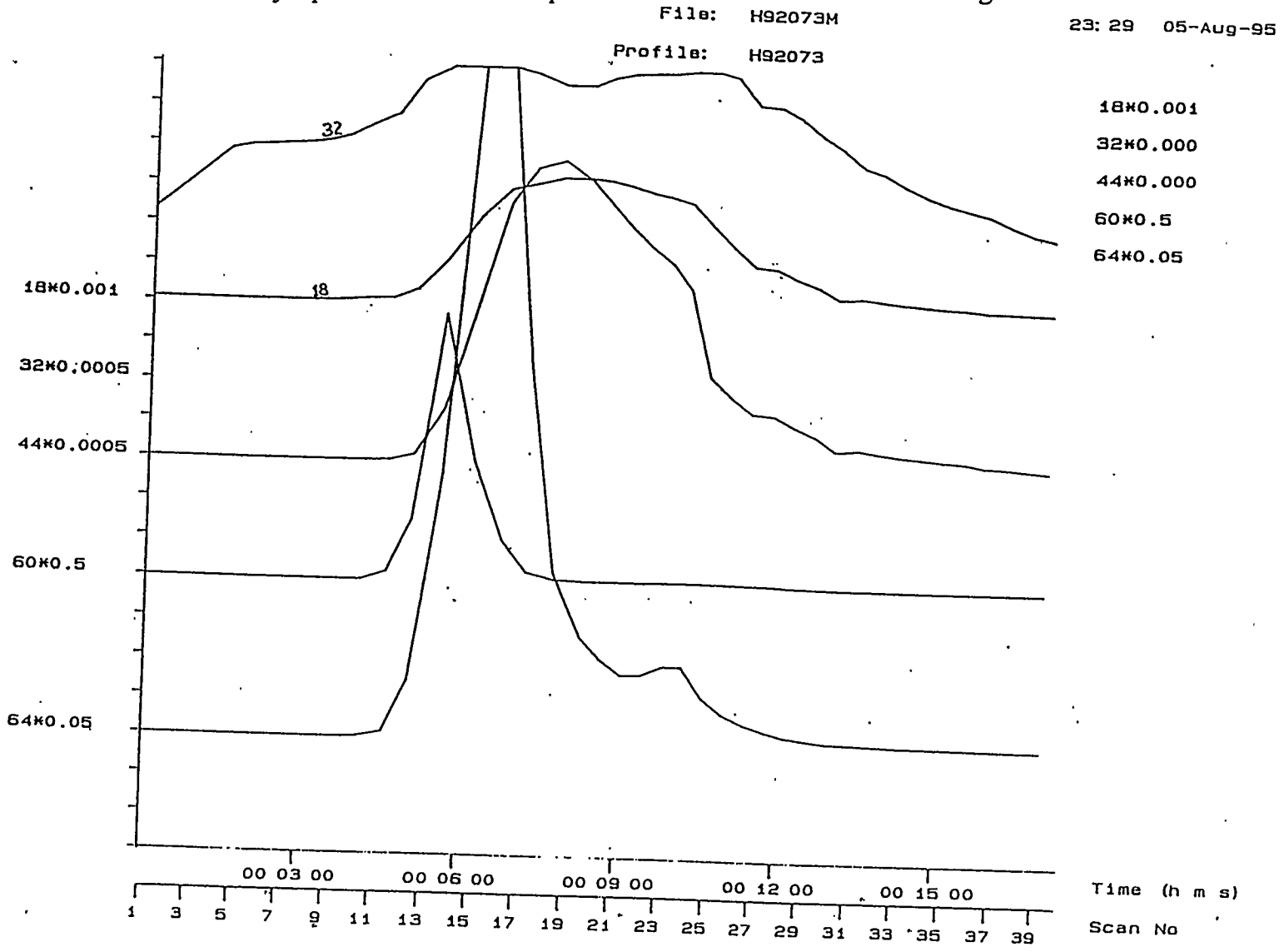

Figure 28. Profiles of some major peaks for combustion products of blend 035122 at the slow heating rate.

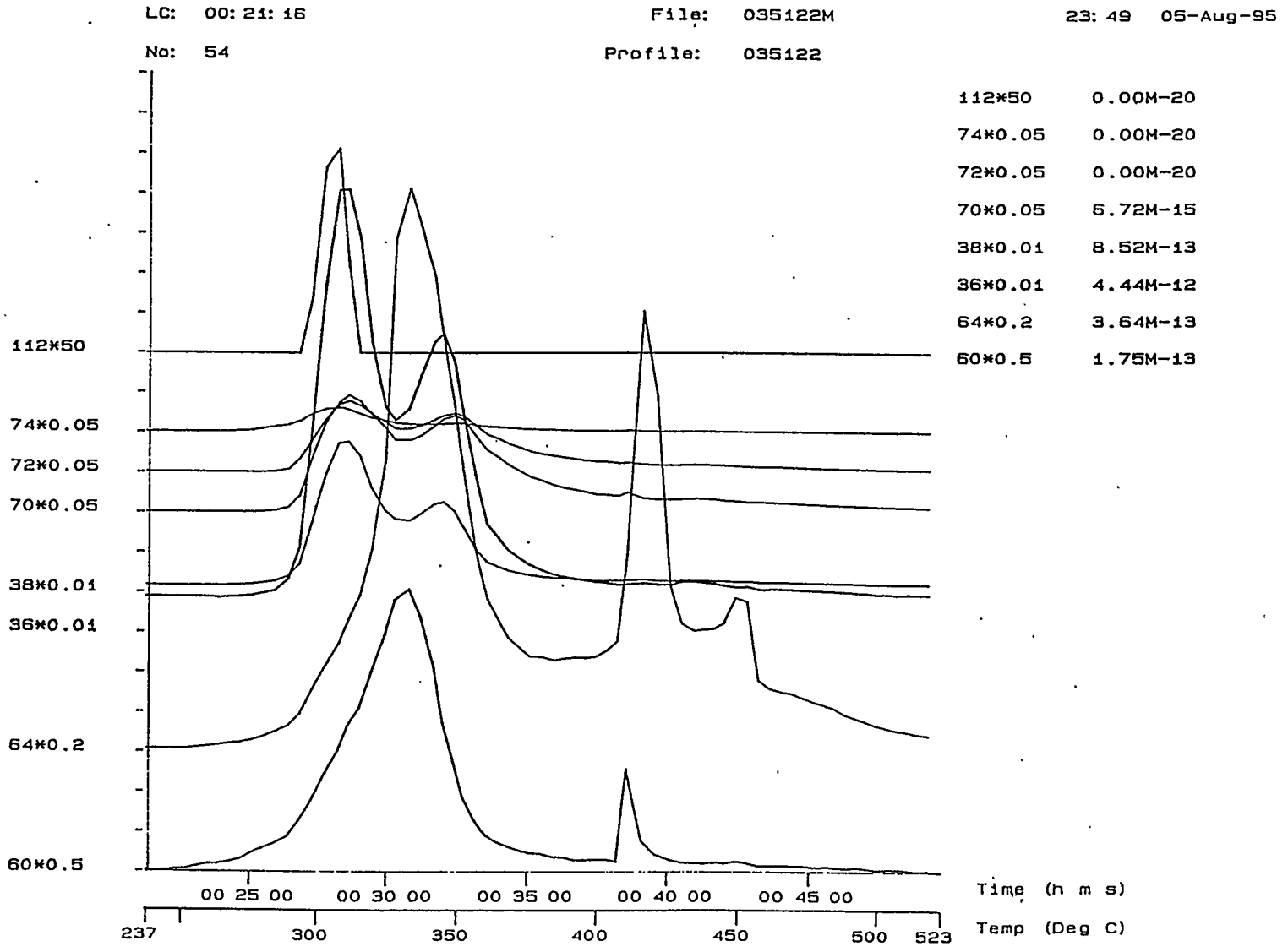

Figure 29. Profiles of some major peaks for combustion products of blend 035122 at the fast heating rate.

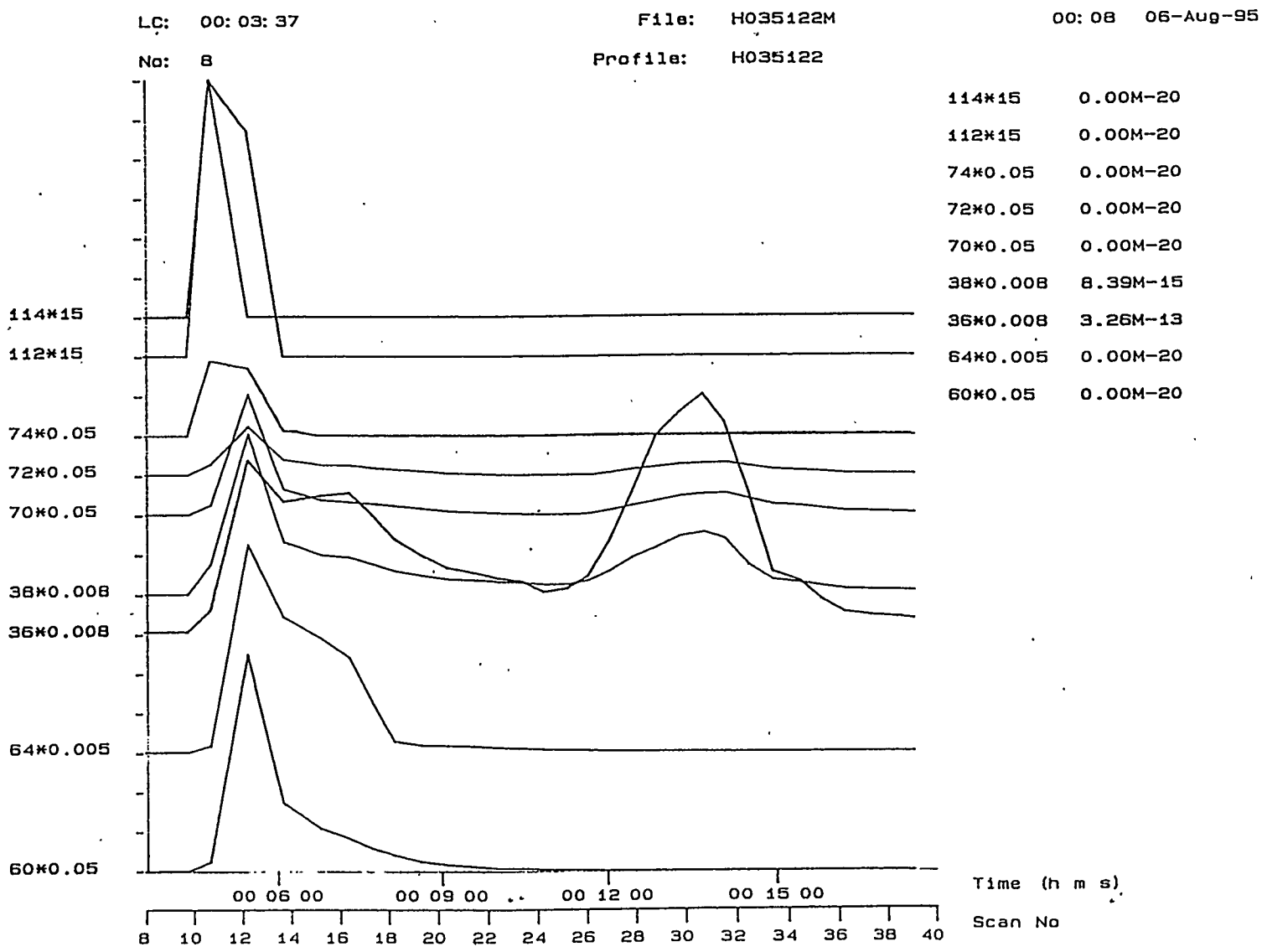

Figure 30. Profiles of some major peaks for combustion products of blend 735122 at the slow heating rate.

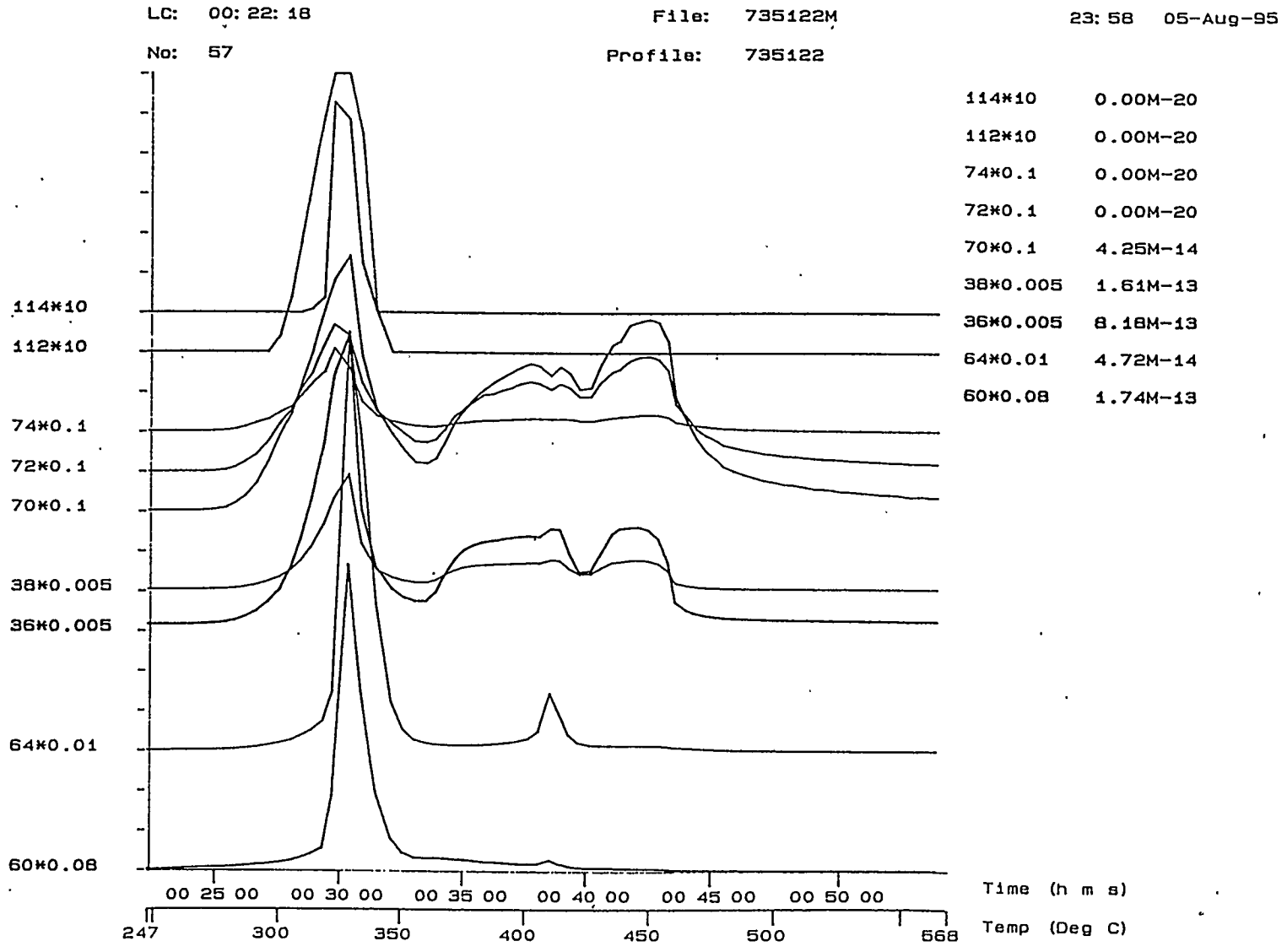

Figure 31. Profiles of some major peaks for combustion products of blend 735122 at the fast heating rate.

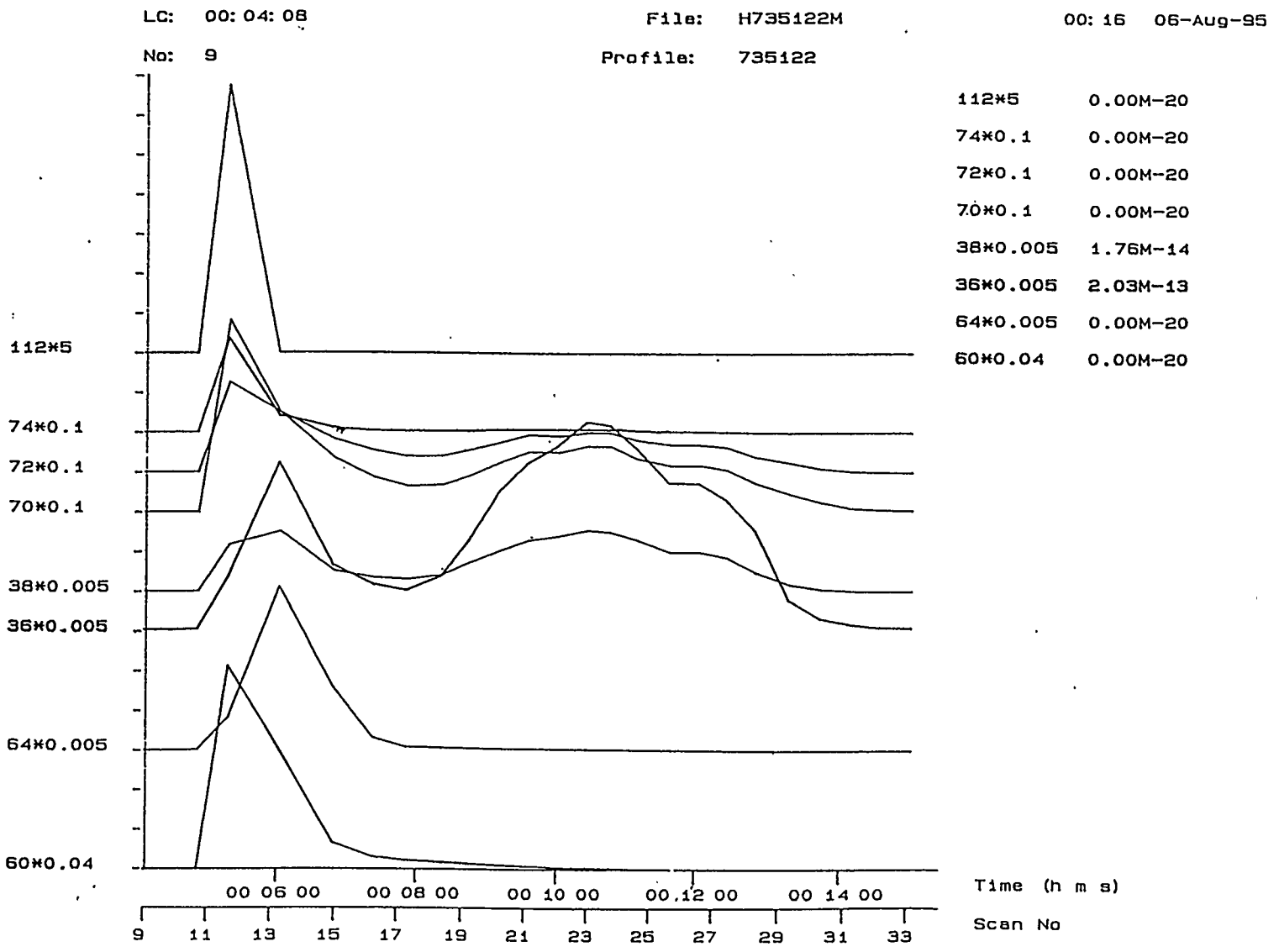

Figure 32. Setup for the trap of the evolutions from coal combustion.